Research article

JGS
Journal of the Geological Society

https://doi.org/10.1144/jgs2020-110 | Vol. 178 | 2020 | jgs2020-110

Linking surface and subsurface volcanic stratigraphy in the Turkana Depression of the East African Rift system

Nick Schofield[1]*, Richard Newton[2], Scott Thackrey[3], Douglas Watson[1], David Jolley[1] and Chris Morley[4]

[1] Department of Geology and Petroleum Geology, University of Aberdeen, Aberdeen 8 AB24 3FX, UK
[2] Tullow Oil plc., 9 Chiswick Place, London, W4 5XT, UK
[3] Total CSTJF, Avenue Larribau, 64000, Pau, France
[4] PTT Exploration and Production, Enco, Soi 11, Vibhavadi-Rangsit Road, 10400, Thailand
NS, 0000-0002-3083-735X
* Correspondence: n.schofield@abdn.ac.uk

Abstract: The Northern Kenya Rift is an important natural laboratory for understanding continental rifting processes. However, much of the current understanding of its geological evolution is based on surface outcrops within footwall highs due to a lack of subsurface geological constraints. In this paper, we present an investigation of the Cenozoic stratigraphy and volcano-tectonic relationship of the volcanic sequences within the Turkana Depression (namely the North Lokichar, North Kerio and Turkana Basins). We integrate regional seismic reflection data collected as part of ongoing petroleum exploration in the area with lithological and biostratigraphic data from new wells that were drilled in 2014 and 2015 (Epir-1 and Emesek-1). This has allowed linking and extrapolation of the detailed stratigraphy of the paleontologically important Lothagam site to the volcanic sequences within the Napedet Hills, North Lokichar, North Kerio and Turkana Basins. The site of the Plio-Pleistocene-age Turkana Fault, which separates the North Lokichar Basin from the Turkana and North Kerio Basins, appears previously to have acted as a focus of Middle Miocene volcanism *c*. 5 Ma prior to the main period of movement on the fault. Our study highlights how subsurface and outcrop information can be combined to give a more in-depth knowledge of the magmatic history within rift basins.

Received 10 June 2020; **revised** 31 August 2020; **accepted** 7 September 2020

The East African Rift system (EARS) (Fig. 1) continues to provide an important natural laboratory to understand rift processes and interlinked volcano-tectonic interactions within sedimentary basins (e.g. Ebinger and Sleep 1998; Morley *et al.* 1999; Vetel and Le Gall 2006; Muirhead *et al.* 2016; Ebinger *et al.* 2017; Ragon *et al.* 2018; Morley 2020). The Turkana Depression, which sits in the eastern arm of the EARS, is important as it represents the most extensively rifted/stretched area of the EARS (with the exception of the Afar Triangle) with the Moho being shallowed to only 20 km depth by extension (Figs 1 and 2) (Hendrie *et al.* 1994; Mechie *et al.* 1997). The Turkana area of northern Kenya has been the site of increased petroleum exploration in recent years due to the discovery of significant petroleum reserves by Tullow Oil and partners within the Miocene Auwerwer Sandstone Formation present within the South Lokichar Basin. Despite continued success, exploration in the region is challenged by the considerable amount of Miocene-to-recent volcanism present within the Kenyan Rift System making seismic reflection imaging of sub-volcanic sequences challenging. Additionally, correlation across the Turkana area and further afield in the EARS is complicated by the sedimentary and volcanic history seen at outcrop within the present-day landscape, as this is often only a partial record that varies depending on local tectonics (McDougall and Brown 2009) with uplift of fault footwalls often eroding large thicknesses of pre-rift stratigraphy. With the increasing amount of subsurface well penetrations and reflection seismic data collected as part of multiple petroleum exploration campaigns, an increased understanding of the surface to-subsurface volcanic stratigraphy between the sub-basins located in the Turkana area can now be elucidated with more control than in previous studies.

The primary aim of this paper is to present an integrated seismic-well-outcrop stratigraphic assessment of the volcanic sequences across the North Lokichar, North Kerio and Turkana Basins, allowing for better constraint of the surface to subsurface volcanic stratigraphy within the Turkana Depression.

Regional structure of the Turkana Rift

Overview of EARS rifting and volcanism

The EARS is a 50–150 km wide elongate north–south system of normally faulted basins that extends for *c*. 3500 km (Fig. 1) (Baker *et al.* 1972; Ebinger 1989) and can be subdivided into eastern and western branches. The eastern branch forms the Kenyan and Ethiopian Rifts, in which NW Kenya sits within an area commonly referred to as the Turkana Depression (Figs 1 and 2). The basins developed in northern Kenya have a width of over 150 km across and are composed of over 30 half-graben basins, commonly bounded by a series of easterly dipping faults (Figs 1–3) (Morley *et al.* 1992, 1999). The Turkana Depression is located between the topographic highs of the East Africa Plateau to the south, and the Ethiopian Plateau to the north (Fig. 1) (Furman *et al.* 2004). Unlike other areas of the EARS, rifting within the Turkana Depression area began when part of the Central Africa Rift system (CARS) formed in the area during the Cretaceous (Morley *et al.* 1999; Furman *et al.* 2006; Boone *et al.* 2019), with further rifting related to both the CARS and the EARS taking place in the Paleogene and Miocene-to-recent, leading to a cumulative Beta factor approaching two (calculated from integration of seismic reflection data, refraction data and modelling) (Ebinger and Ibrahim 1994; Hendrie *et al.* 1994).

Morley *et al.* (1999) provide a geological history of the EARS with particular respect to Kenya and the Turkana region, based on

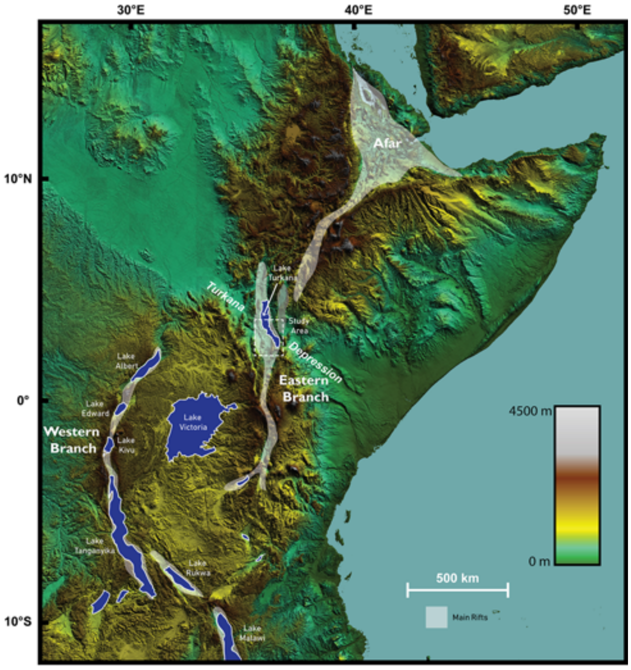

Fig. 1. Topographic shaded relief map showing the East African Rift (EAR). The study area of this paper within the Turkana Depression is marked. Topography data from SRTM (Shuttle Radar Topography Mission) one arcsecond dataset.

well results from the early exploration phase in the 1990s and regional seismic reflection lines collected as part of petroleum exploration. For consistency, the general structural framework presented by Morley *et al.* (1999) and names of individual fault segments are adopted where possible within this paper (e.g. Fig. 4)

Structure of the Southern and Northern Lokichar Basins

The Lokichar basins comprise north–south trending, 30×120 km, broadly half-graben geometry (Morley *et al.* 1992, 1999). The sedimentology, geochemistry and basin development have been described by Morley *et al.*, (1999), Talbot *et al.*, (2004) and Tiercelin *et al.*, (2004, 2012*a*, *b*). Distribution of normal displacement along the main bounding fault of the South and North Lokichar half-grabens shows a remarkable temporospatial evolution where the North Lokichar Basin is notably younger than South Lokichar with the South and North Lokichar Basins being separated by a broad intra-basin high (Morley *et al.* 1999). Segmentation of the Lokichar Fault into three main sections is clearly visible on gravity data, likely reflecting the separate stages of rift progression northwards as well as the potential interaction of the border fault with inherited basement structures (Fig. 3).

Within the South Lokichar Basin, the main phase of rifting commenced during the Late Oligocene to Early Miocene, with rifting ceasing into the late Middle Miocene, with the basin then transitioning into a post-rift sag stage which resulted in deposition of a thin Upper Miocene-to-recent fill (see Loperot-1 in Fig. 18) (Morley *et al.* 1999; Vetel *et al.* 2004; Vetel and Le Gall 2006; Boone *et al.* 2019). However, the North Lokichar Basin illustrates a contrast in rift timing where, based on data from Emesek-1 (this paper), the syn-rift package is composed of *c.* 2 km of Upper Miocene shale and sandstones (see Emesek-1 in Fig. 18), much younger than the syn-rift package in South Lokichar. The presence of the Middle Miocene volcanic sequences with the North Lokichar Basin makes discrimination of any earlier rifting events (e.g. Late Oligocene to Early Miocene) difficult to constrain in detail, due to degradation in seismic reflection imaging below the volcanic sequences.

Structure of the North Kerio and Turkana Basins

The North Kerio Basin (Fig. 3), lies east of the Napedet (known in Kenya locally as Napudet), Kamutile and Auwerwer Hills and is bounded to the west by a series of easterly dipping faults, including the Lokhone Fault, Napedet Fault and Lothagam Fault, which forms a prominent fault escarpment that bounds the uplifted footwall block of Lothagam (Fig. 3).

The Lothagam Fault bounds one of a series of westerly dipping sub-basins formed by north-trending en-echelon faults which trend northwards away from the present-day Kamutile Hills (Fig. 3) (Morley *et al.* 1992) and marks the juxtaposition point of the North Kerio Basin and the southern extent of the Turkana Basin. Although ostensibly regarded as separate basins, both the North Kerio Basin and southern Turkana Basin are thought to share a similar rifting history (Morley *et al.* 1999; Vetel and Le Gall 2006).

Volcanism across the Turkana Depression

Volcanism within the EARS is thought to have begun in Ethiopia around the Middle Eocene (45 Ma) (Davidson and Rex 1980; Ebinger and Ibrahim 1994; Hendrie *et al.* 1994; George *et al.* 1998; Furman *et al.* 2004; see the review in Rooney 2017). The geodynamic origin of the volcanism across the EARS has been subject to much debate (Rooney 2020), with arguments for the presence of a single plume (Ebinger and Sleep 1998), or multiple plumes (George *et al.* 1998; George and Rogers *et al.* 2002) influencing the development of the EARS. Across the Turkana Depression, volcanism commenced in the Eocene around *c.* 39 Ma with eruption of up to 3 km of extrusive volcanics thought to have emplaced over much of the Turkana Depression as a result of intense fissure eruptions from the Late Eocene to Middle Miocene (Morley, 1994; McDougall and Brown 2009; Ragon *et al.* 2018). Within southern Turkana (e.g. South Lokichar), this episode is largely absent. Locations of volcanic activity within the Turkana area have shifted since the Eocene–Oligocene to the Plio–Pleistocene. During the Early Oligocene (33.9–27 Ma) volcanism occurred in the NW and central area of the Turkana depression, in the region of the Lotikipi Plain (Songot-Mogila and Moruerith-Kalin volcanics) and within the Muruanasigar area (Pelekech volcanics) *c.* 100 km to the west of the present-day central Lake Turkana (Rooney 2017). During the Early Miocene (26.9 Ma–22 Ma) a resurgence phase took place (Rooney 2017) with volcanism occurring on both sides of the central Lake Turkana area (including the Lothidok ranges) (Rooney 2017). From the Mid-to-Late Miocene (15–6 Ma) volcanism shifted once more to southern and NE Turkana (including the Napedet–Kamutile–Kathigithigiria Hills area and Lothagam), and Lake Turkana to eastern Turkana during the Plio–Pleistocene (see the review in Morley 2020).

Data and methodology

Seismic and gravity data

An extensive 2D seismic reflection database was available across the North Lokichar, North Kerio and Turkana Basins; this database consisted of older legacy lines supplemented by newer lines collected by Tullow and Partners between 2010 and 2012. All data are displayed in two-way-time (TWT) (Fig. 4). Full-tensor gradiometry maps were also available, which helped define some of the major structure in the area and delineate faults (e.g. the Lokichar Fault) which have no surface expression (Fig. 3).

Wells

Three wells were used in this study; Emesek-1 (North Lokichar Basin), Epir-1 (North Kerio Basin) and Eliye Springs-1 (Turkana Basin). The primary focus of analysis was on the more recent

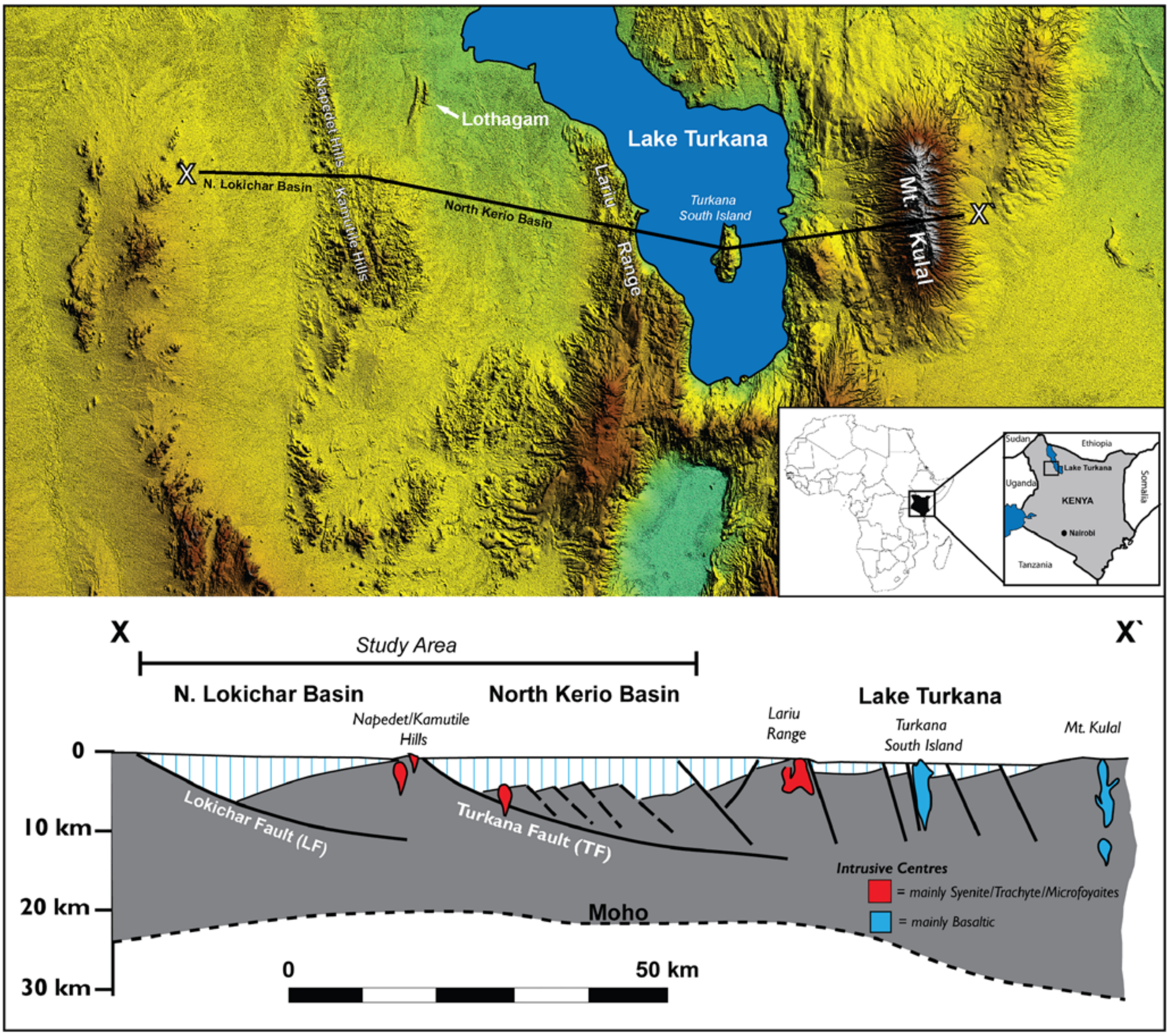

Fig. 2. Schematic crustal cross section across the study area (modified from Morley *et al.* 1999), showing the half-graben nature of the North Lokichar and North Kerio Basin. Of particular note are the intrusive centres which occur within the Napedet/Kamutile Hills. Topography data from SRTM one arcsecond dataset.

Emesek-1 and Epir-1 wells (drilled in 2014/15) due to the quantity of data acquired and relevance to outcrop exposures. The Eliye Springs-1 well (drilled in 1992 by Shell; Morley *et al.* 1999) has comparatively limited data but is nonetheless a critical control point regionally (Figs 3 and 4). Throughout the paper and in the figures, depths are quoted in mBRT (metres below rotary table).

It is important to note that lithological and petrophysical descriptions of volcanic sequences within petroleum wells are often fraught with errors and incorrect interpretations, particularly those derived at wellsite (Millett *et al.* 2016; Watson 2019). In general, logging of volcanic lithologies is an uncommon occurrence within petroleum exploration, with rare exceptions where igneous rocks act as reservoirs to hydrocarbons. This is because wells avoid penetrating igneous rocks, due to issues with seismic imaging (Ziolkowski *et al.* 2003), slow drilling rates and drilling hazards associated with fractured rocks (Millett *et al.* 2016; Schofield *et al.* 2020). This aspect has led to a general lack of exposure of wellsite loggers and petrophysical interpreters to volcanic lithologies within the subsurface, which can lead to a radically different interpretation of volcanic sequences. Both Emesek-1 and Epir-1 were re-logged and interpreted as part of this study to bring them into a correct volcanological and stratigraphic context. An example of the errors that can occur in taking composite logs (i.e. basic wireline logging information and lithological interpretation displayed together) from petroleum wells as accurate representations of subsurface volcanic lithologies penetrated is demonstrated by the Emesek-1 well (Fig. 5). On the original composite log, the volcanic section in Emesek-1 had been interpreted to consist of 1340 m of mostly tuffaceous claystone and volcanic sandstone (Fig. 5). However, upon re-logging, utilizing petrophysical data, side wall core (SWC) and cuttings, the volcanic sequence was found to be instead: (1) 781 m thick (v. 1340 m), (2) the depth of the top of volcanic sequences was 274 m lower that the original log, (3) the base of the volcanics was 285 m higher than the original log, and (4) the 'tuffaceous claystone' interpreted in the original log was actually composed of both basaltic and dacitic lava flows. No evidence of tuff was found within the volcanic section when analysing the cuttings or SWCs.

Eliye Springs-1 provided limited scope for detailed analysis, as only the final well report (which summarizes the drilling results), biostratigraphic report and composite log were available during the evaluation, but the well was examined in detail by Morley *et al.* (1999). Therefore, interpretation has been based on the data from the

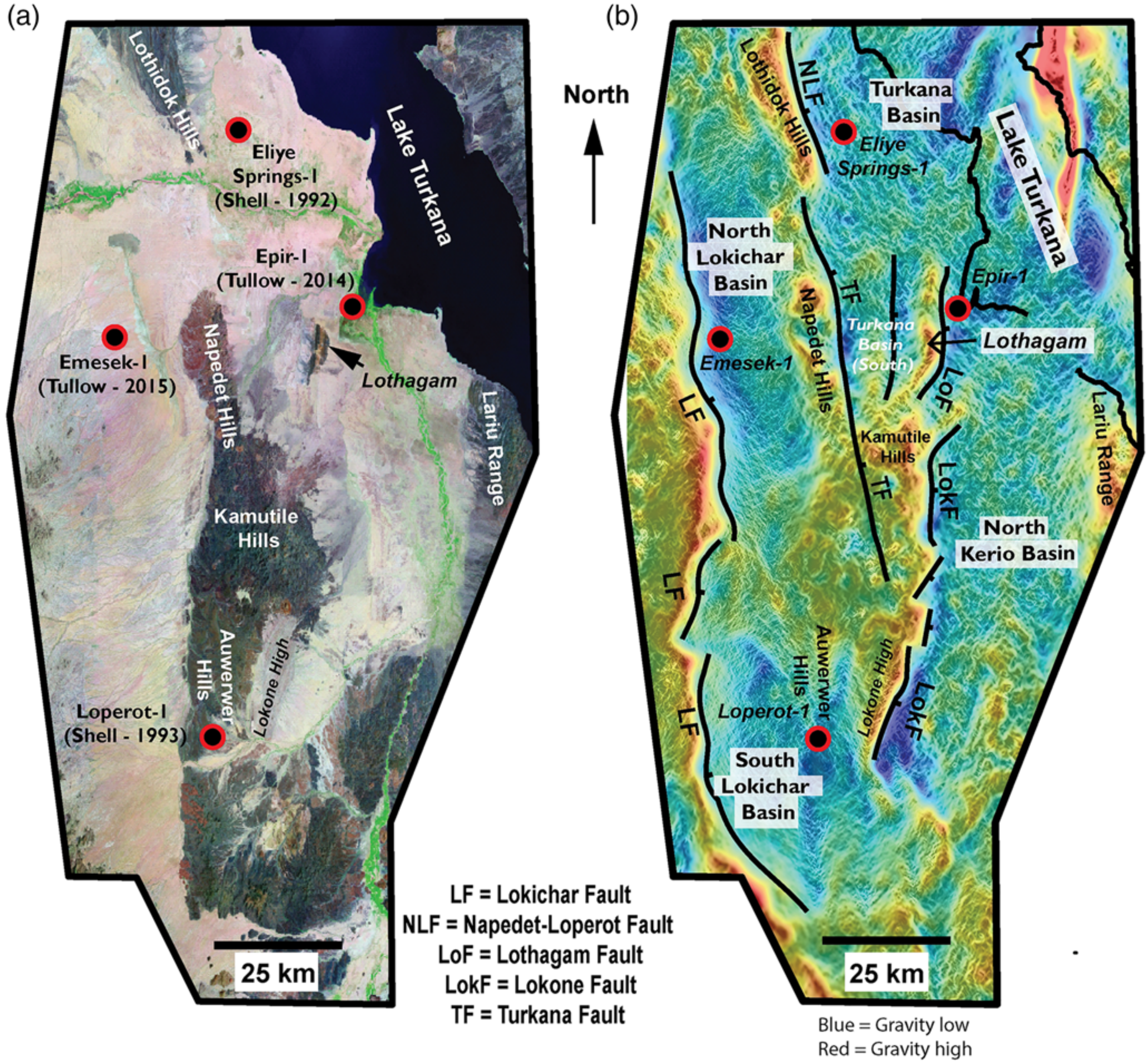

Fig. 3. (**a**) Landsat image showing main features within study area and location and year of drilling of key exploration wells referred to throughout this paper. (**b**) Full-tensor gradiometry map showing main structural framework and basins referred to in this study. Note the clear occurrence of the Lokichar Fault, and its separate fault segments, which have no surface expression.

final well report and composite log, in conjunction with the broad stratigraphic relationship which can be discerned from seismic interpretation and seismic correlation.

It is important to note that, due to ongoing petroleum exploration (as of 2020) and the importance of both the Emesek-1 and Epir-1 wells to understanding of the petroleum systems within northern Kenya, petroleum aspects of the wells and area are not discussed in detail within this paper.

Stratigraphy of sedimentary basins and hill ranges in western Turkana

South Lokichar Basin

Within the South Lokichar Basin, Proterozoic basement (exposed in the present day within the Lokhone High) is overlain by the Paleogene to Early Miocene Loperot Formation (see Loperot-1 in Fig. 18), which consists of a series of fluvio-deltaic sandstones interfingered with two important petroleum source rock sequences: the Lokone and Loperot shale members (Morley *et al.* 1992). Overlying this formation is the Middle Miocene Auwerwer Sandstone Formation, which contains a considerable component of volcaniclastics and reworked volcanics, which possess a strongly silica-undersaturated alkaline composition (Tiercelin *et al.* 2004). Immediately capping this unit is the Middle Miocene tabular lava flows of the Auwerwer Basalts (see Loperot-1 in Fig. 18), named after the Auwerwer Hills, which form a prominent topographic range in the South Lokichar Basin, and extend to the north where the range merges into the Kamutile and Napedet Hills (Fig. 3).

North Lokichar Basin (Emesek-1)

The exact stratigraphy of the North Lokichar Basin has remained somewhat enigmatic, aside from interpretation of legacy seismic lines which illustrated the younger Miocene-to-Pliocene age of the basin, and potential occurrence of a Middle Miocene volcanic sequence (Morley *et al.* 1992; Morley *et al.* 1999). The drilling of the Emesek-1 well within the North Lokichar Basin therefore provides an important subsurface datapoint. The stratigraphy of the

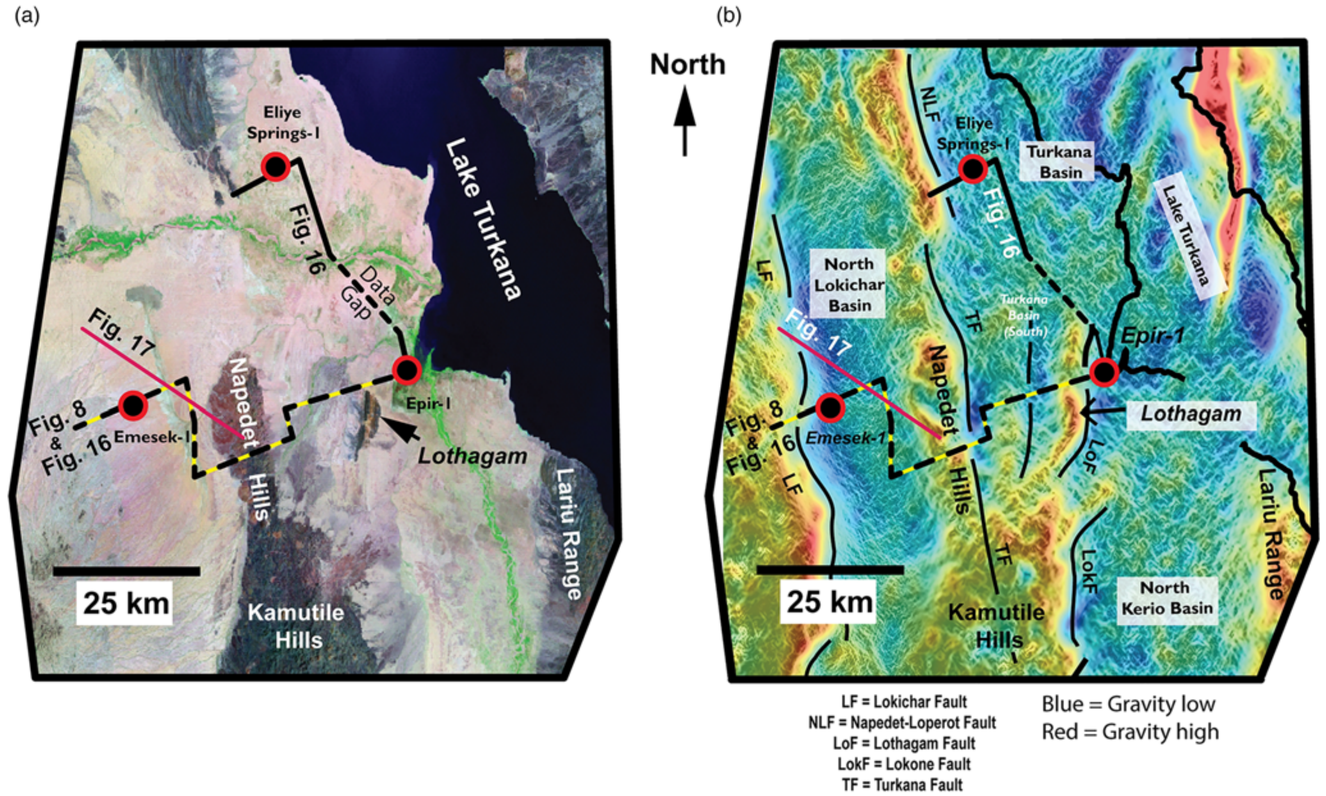

Fig. 4. Map showing location of seismic lines used within this study.

volcanic section penetrated by Emesek-1 is given in detail within Figure 6.

After substantial success of petroleum exploration within the South Lokichar Basin, the Emesek-1 well was drilled in 2015 by Tullow Oil plc with partner Africa Oil Corp. to test the prospectivity of an upthrown intra-basinal fault block within the North Lokichar Basin. Upon drilling, the well encountered *c.* 1900 m of Plio–Pleistocene to Upper Miocene sedimentary rocks. At 1932 mBRT, the well encountered a *c.* 700 m thick unit consisting of mainly extrusive volcanics, before penetrating a *c.* 240 m sub-volcanic clastic sequence, containing minor amounts of primary volcanic clasts. The well reached a total depth (TD) of 3000 mBRT.

The volcanic package intersected at 1932 mBRT (Fig. 6), commenced with a 83 m thick package of basaltic tabular lava flows, separated by thin claystone horizons. At 2015 mBRT a 155 m thick claystone and siltstone package with occasional volcaniclastic sandstone units was intersected. From 2170 mBRT, a 136 m thick unit of basaltic lava and volcaniclastic horizons occurs. Two sill intrusions were penetrated between 2340 mBRT to 2392 mBRT; the upper sill penetrated is doleritic in composition (basic), but the lower sill is composed of more evolved aphyric diorite (intermediate), as confirmed from a sidewall core and wireline log character, which are characteristic of a compositionally intermediate intrusion (Fig. 7; see Mark *et al.* 2018). A 178 m thick mixed assemblage of lavas, volcaniclastic sandstone and siltstone occurs from 2392 mBRT, with palynological analysis showing potential upland input of sediment into this interval. A sharp log change in gamma ray occurs at 2570 mBRT, marking a unit which consists of a 79 m thick series of evolved dacite lavas (Figs 6 and 7). The base of the volcanic sequence, from 2649 mBRT to 2713 mBRT consists of a 64 m thick succession composed of classic basaltic tabular lava flows interbedded with volcaniclastic sandstone and siltstones.

At 2713 mBRT to TD of the well at 3000 mBRT, the well penetrated a 245 m thick interbedded sandstone and siltstone section (Fig. 8), which contained sparse evidence of primary (i.e. early generation) volcanically derived material. From the base of the well to the base of the volcanic sequence, palynology indicates a shallowing of water depth from eutrophic lake conditions in a potentially distal lacustrine setting, to a lacustrine margin, prior to eruption of the volcanics (Fig. 6).

Within the Emesek-1 well, no other basalt lavas were encountered within the Upper Miocene and Plio–Pleistocene sections which overly the Middle Miocene volcanics. This implies the *c.* 4 Ma Gombe basalts did not reach the area of the North Lokichar Basin (Haileab *et al.* 2004).

North Lokichar Basin (Napedet Hills and Kamutile Hills)

The Napedet Hills area is formed from the exposed up-dip hanging wall of the North Lokichar Basin and footwall block of the Turkana Basin (south) (Figs 3, 8 and 9), being bounded by the Turkana Fault. The hills expose an array of volcanic rocks, composed of basaltic lava flows, phonolites, dyke swarms and igneous centres (Fig. 10) (Dodson 1971; Morley 2020). Limited K–Ar whole rock dating from the area indicates an age range for the lava flows from *c.* 15 Ma to 12.8 Ma (Morley *et al.* 1992; McDougall and Brown 2009). The phonolite lavas form isolated exposures capping underlying basalts and volcaniclastics (Fig. 10) (Dodson 1971). Intruded into the Napedet Hills are a series of microfoyaite igneous plugs/centres (Fig. 10) , which are classified by Dodson (1971) on texture, with microfoyaite referring to an intermediate texture between phonolite and the equivalent plutonic rock (nepheline syenite). In the Kamutile Hills an intrusive complex is exposed (*c.* 8 km long in a north–south direction), which includes radial and concentric dyke patterns (Morley 2020). From seismic lines that cross the Napedet Hills to Emesek-1 (Fig. 8), it is apparent that the present-day exposure of the volcanics sequences within the Napedet Hills represents a heavily eroded and truncated sequence of the volcanics which form the same broad stratigraphic unit penetrated

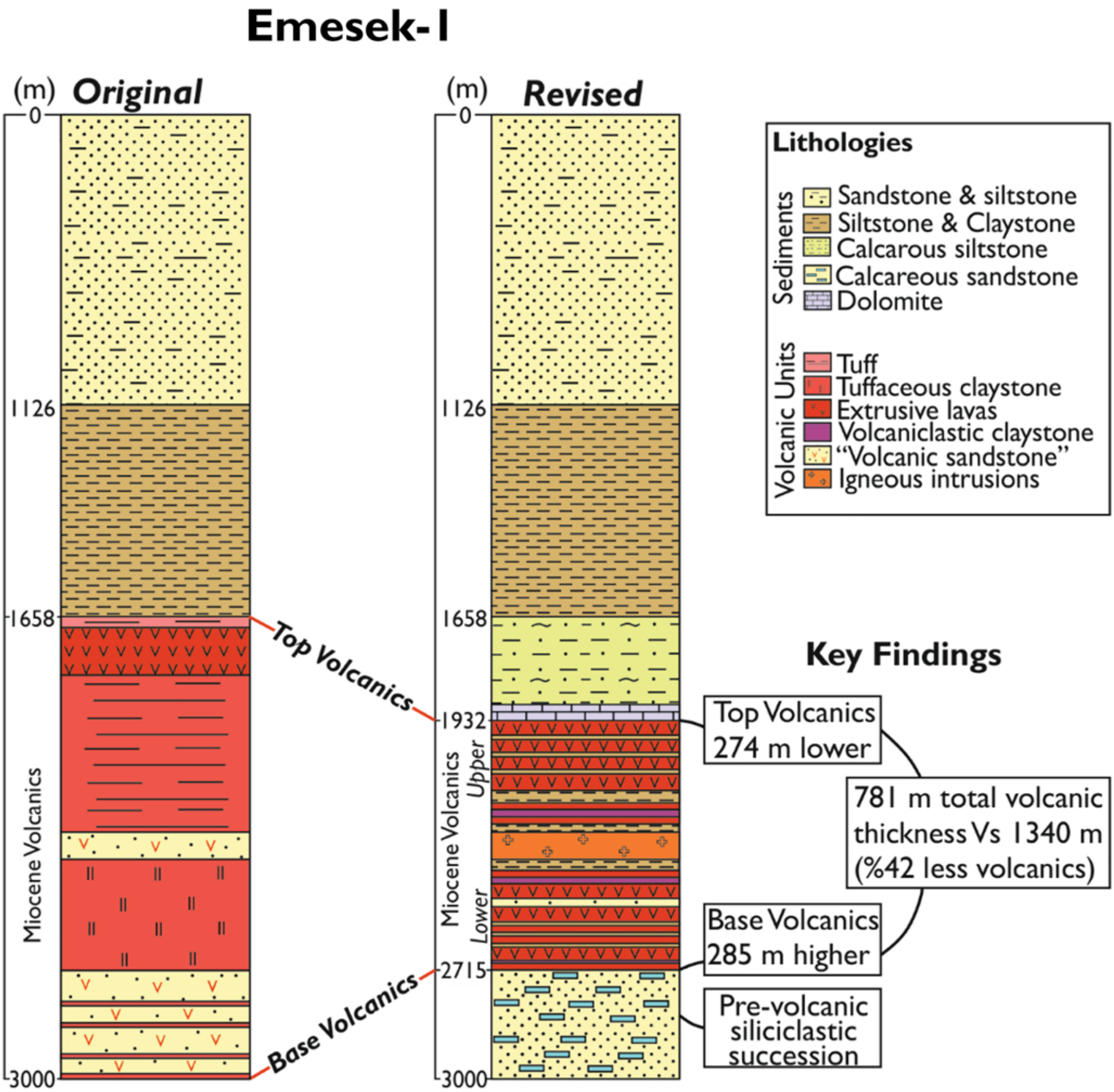

Fig. 5. Figure showing the original interpretation of the volcanic section within the Emesek-1 well v. the revised log interpretation, which was based on full petrophysical, cuttings and side wall core analysis. The figure highlights the care which needs to be exercised when taking composite well logs from petroleum wells as accurate representations of subsurface geology when dealing with volcanic sequences.

down-dip by the Emesek-1 well. The erosion of *c.* 300–500 m of volcanic material, presumably a result of footwall uplift during Plio–Pleistocene rifting in the adjacent Turkana Basin, appears to have taken place in the Napedet Hills. This suggests that the phonolite flows that sit upon the underlying basalt, and that currently form isolated exposures within the Napedet and Kamutile Hills, were substantially more aerially extensive than is currently exposed. It seems probable that the now exposed microfoyaite centres and dyke swarms, as visible within the Napedet Hills and NE of the Kamutile Hills (Fig. 10), likely represented the intrusive feeding system to the extrusive phonolite flows.

Turkana/North Kerio Basin (Lothagam)

One of the most striking features within the North Kerio Basin is the prominent topographic feature of Lothagam (referred to as Lothagam Hill in the early literature), which is located 15 km to the east of the Napedet Hills and rises *c.* 200 m above the desert floor (Figs 3, 11 and 12). Lothagam represents the tilted footwall block of the Lothagam Fault which bounds the westerly margin of the North Kerio Basin (Fig. 10), exposing a section of Miocene-to-Pliocene-aged volcanic and sedimentary rock in an area *c.* 10 km long by 3 km wide (Figs 11 and 12). The footwall area of Lothagam has received a considerable amount of research over the last 40 years, because it represents one of the most important sites on the African continent for studying vertebrate evolution during the Miocene-to-Pliocene and contains one of the oldest known hominid fossils (*c.* 5 Ma) (Fig. 12a) (Leakey and Walker 2003). The stratigraphy of Lothagam has been studied in more detail than any other area in Turkana and is subject to several different nomenclatures as highlighted by McDougall and Feibel (1999) and Feibel (2003). The most recent and detailed nomenclature is that of Powers and Feibel (unpublished data reported in Leakey *et al.* 1996; McDougall and Feibel 1999; Feibel 2003; Fig. 12a) and it is

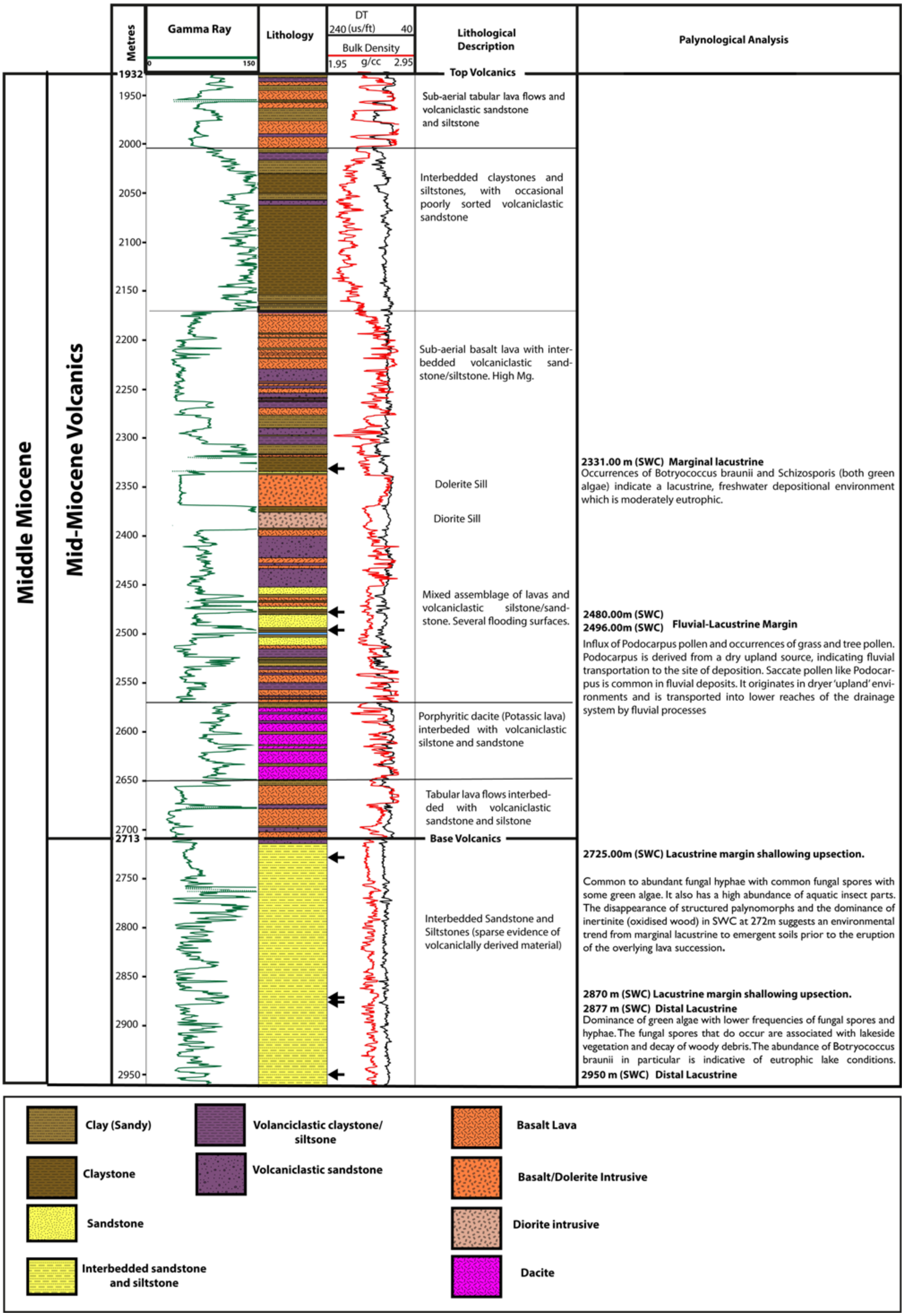

Fig. 6. Figure showing the Middle Miocene volcanics penetrated by the Emesek-1 well (drilled in 2015) located within the North Lokichar Basin.

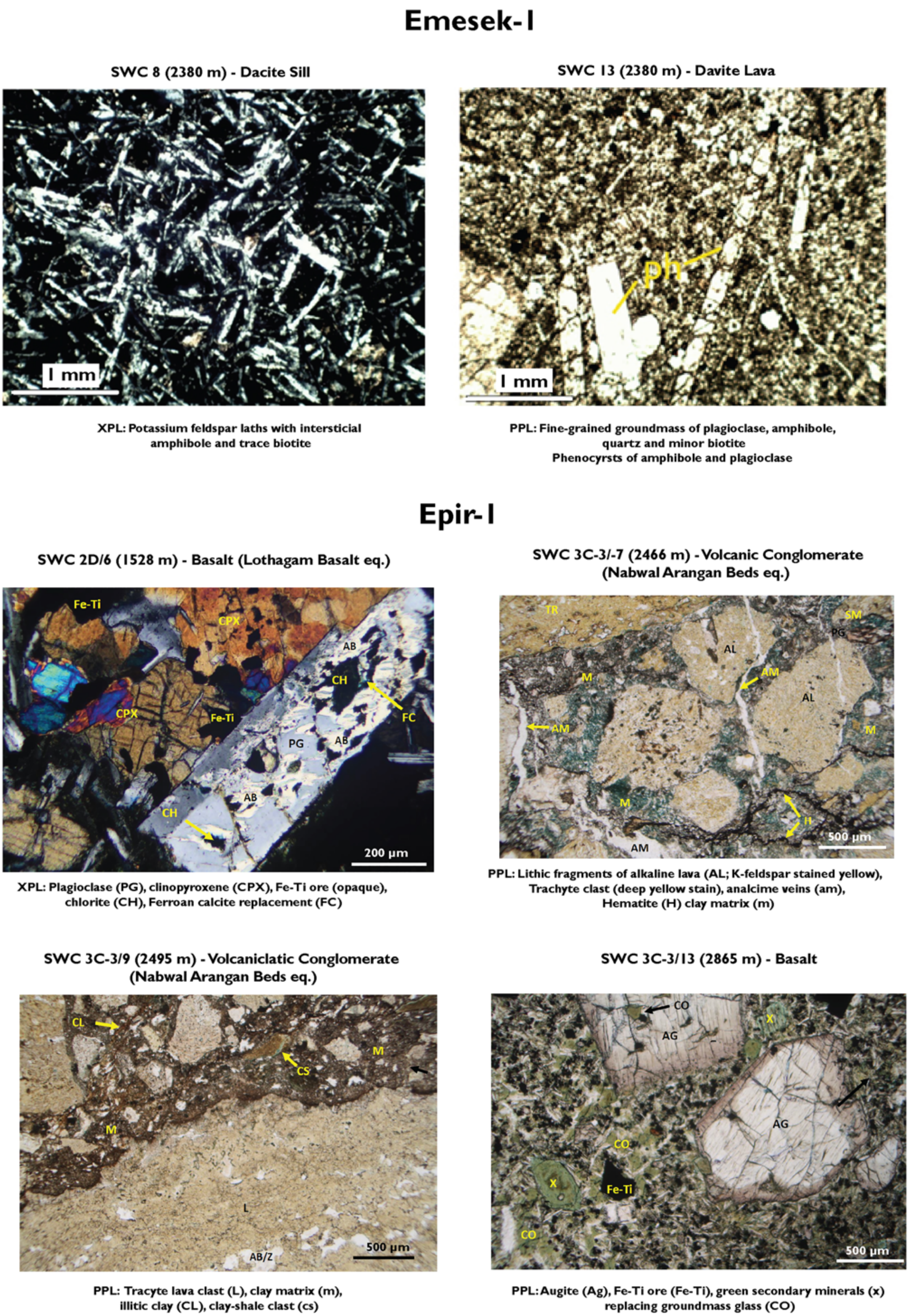

Fig. 7. Assorted thin-section micrographs taken from side wall cores (SWCs) within the Emesek-1 and Epir-1 wells. Depths at which SWCs are taken are listed, as are descriptions of rocks encountered. ALS Petrophysics are acknowledged for Epir-1 petrography.

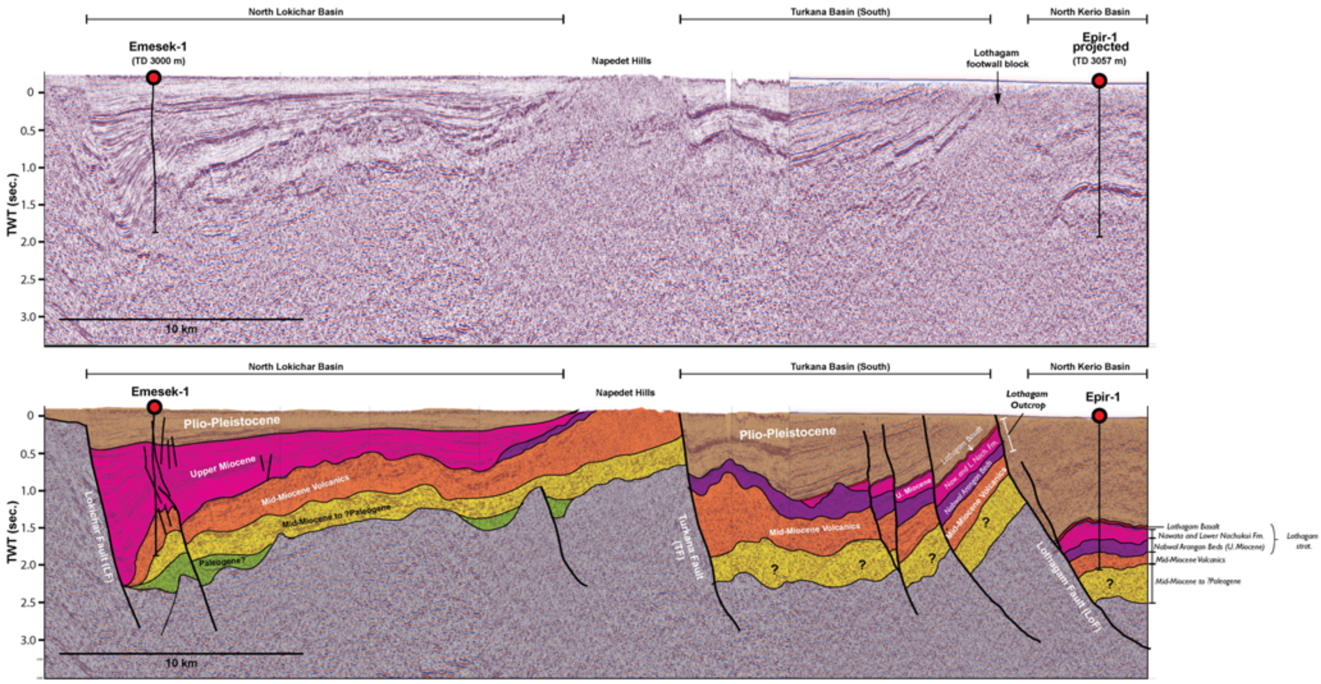

Fig. 8. Seismic line and accompanying geo-seismic interpretation showing main structural and volcanic relationships between the North Lokichar, Turkana (South) and North Kerio Basins. Areas marked with a (?) are those where interpretation is particularly uncertain.

this stratigraphic terminology that is adapted and used within this paper for both Lothagam and the subsurface tie to the equivalent sequences in the Epir-1 well located 7 km NE of Lothagam in the North Kerio Basin (see the next section).

The base of the exposed Lothagam sequence consists of the Middle Miocene Nabwal Arangan beds, which comprise isolated compound phonolite and basalt lava flows (K–Ar dated between *c*. 14–12 Ma) interbedded with proximally derived conglomerate to boulder volcaniclastic debris flows that occasionally grade into stream flows (McDougall and Feibel 1999) (Figs 12–14). The unit, which shows a variety of volcanic compositions (e.g. phonolite, trachyte, basalt), suggests a very active period of erosion of the volcanic landscape in the Turkana area during the Middle Miocene, which culminated in deposition of proximal alluvial fan-type deposits (Figs 13 and 14). A basalt at the top of the Nabwal Arangan beds has been dated at 9.1 ± 0.2 Ma (McDougall and Feibel 1999; Figures 11 and 12a). The overlying Nawata Formation is composed of a heterogenous mix of fining upward fluvial sandstone to mudstone deposits, interspersed with conglomerates and tuff horizons (McDougall and Feibel 1999; Feibel 2003). The age of the formation is estimated to be between 8 Ma and 5 Ma (McDougall and Feibel 1999). Overlying the Nawata Formation is

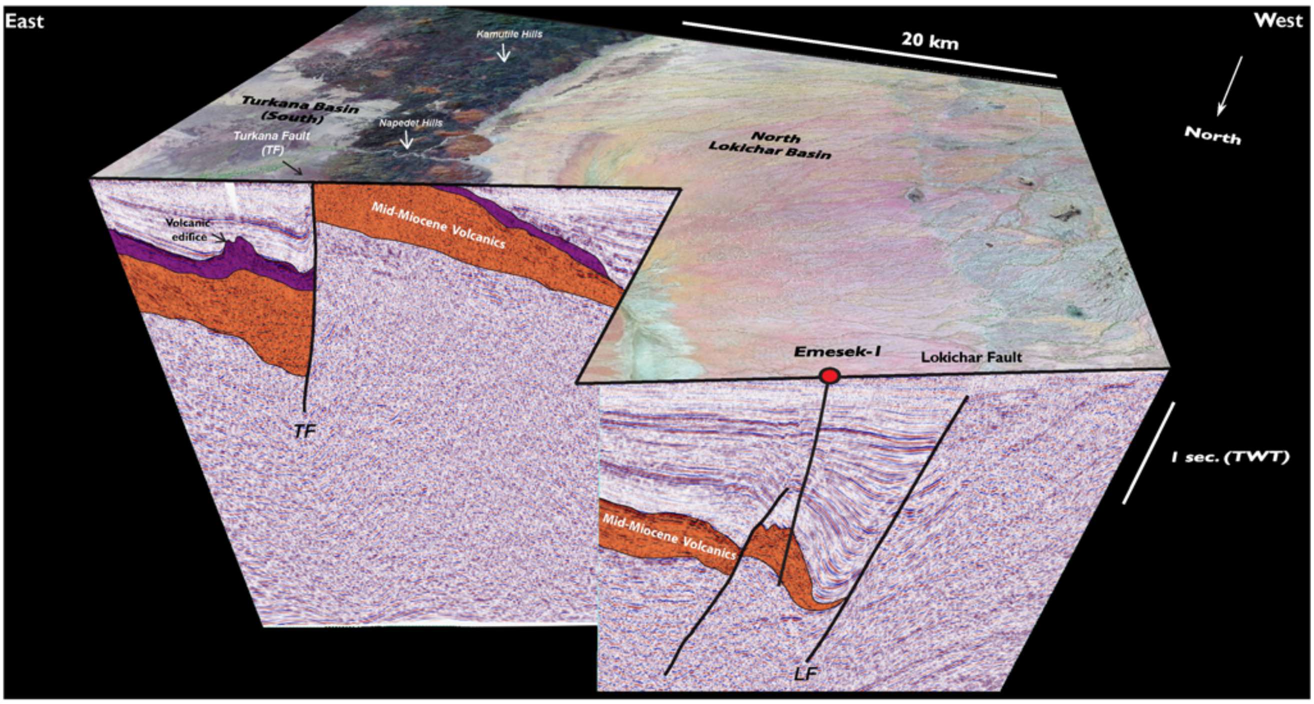

Fig. 9. Oblique cutaway view of the North Lokichar Basin based on Landsat imagery, showing the Middle Miocene volcanic penetrated by Emesek-1 outcropping in the Napedet Hills.

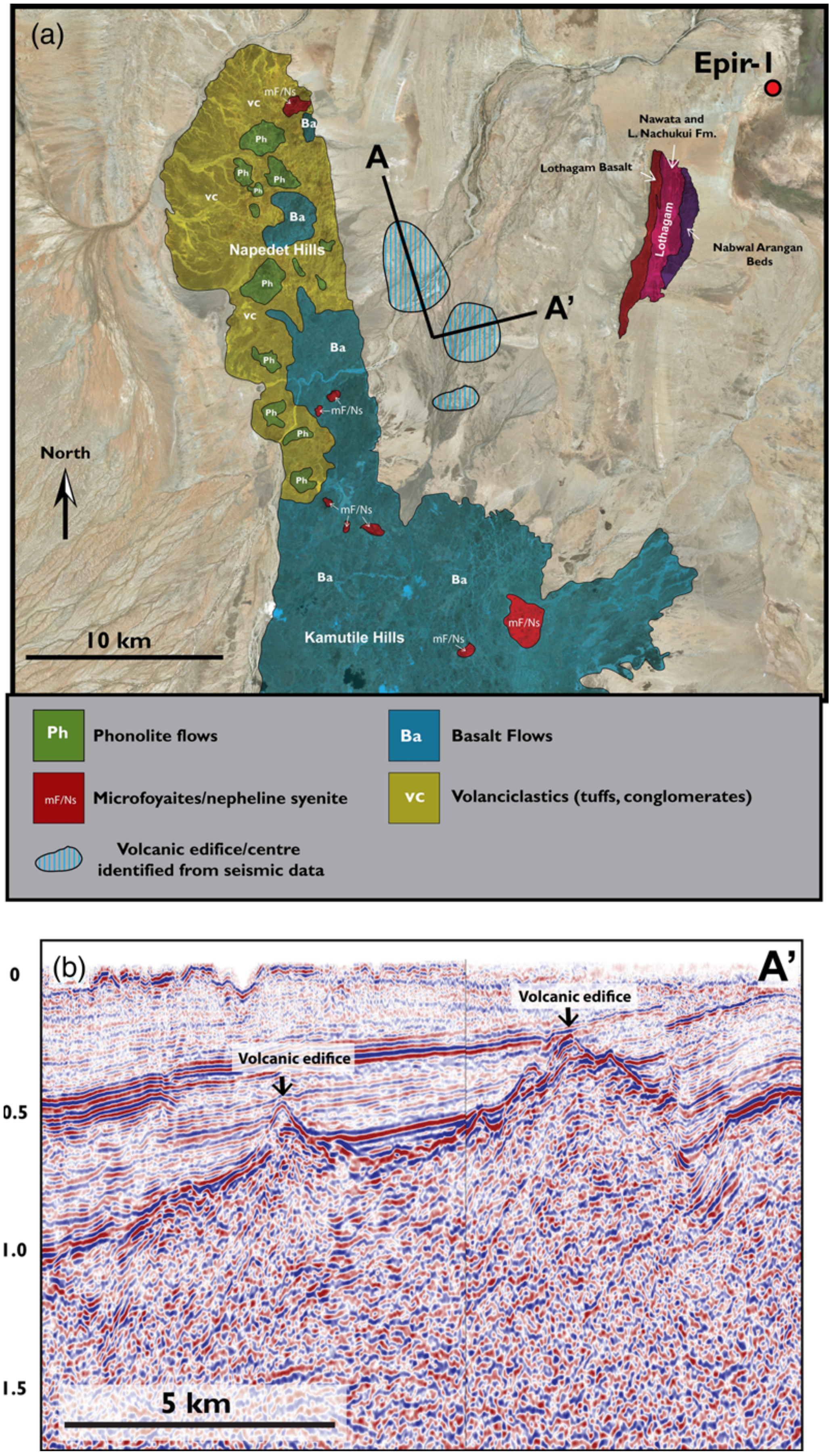

Fig. 10. (**a**) Geological sketch map (modified from Dodson 1971) overlain on a Landsat image. The Napedet and Kamutile Hills contain a series of basalts which are capped in isolated outcrops by phonolite lava flows. A series of microfoyaites/nepheline syenite intrusive centres occur throughout the hills but are particularly concentrated within the Kamutile Hills. (**b**) Seismic line through two volcanic edifices now buried within the subsurface, but which are part of the same volcanic sequence exposed within the Napedet and Kamutile Hills.

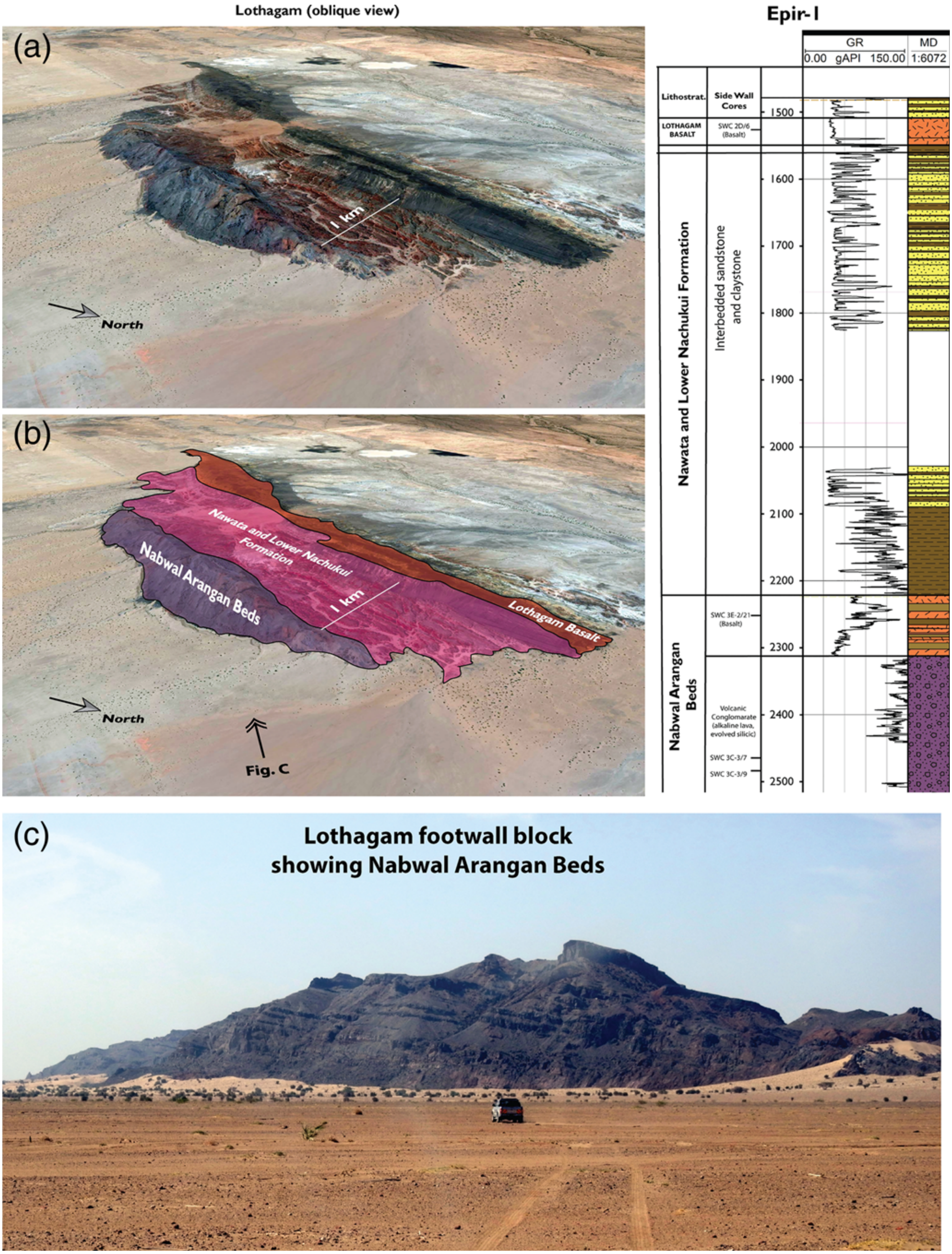

Fig. 11. Figure showing the Lothagam tilted footwall block which rises from the desert floor of the North Kerio Basin by *c*. 200 m. (**a**) Oblique view of Lothagam looking SW of a Landsat image draped over SRTM topographic data. (**b**) Oblique view of Lothagam with stratigraphy of Powers and Feibel (in Leakey *et al.* 1996) overlain. (**c**) Field photograph looking SW, direction marked in (**b**), showing the Nabwal Arangan beds of Lothagam; note the shallow tilt of the beds to the east.

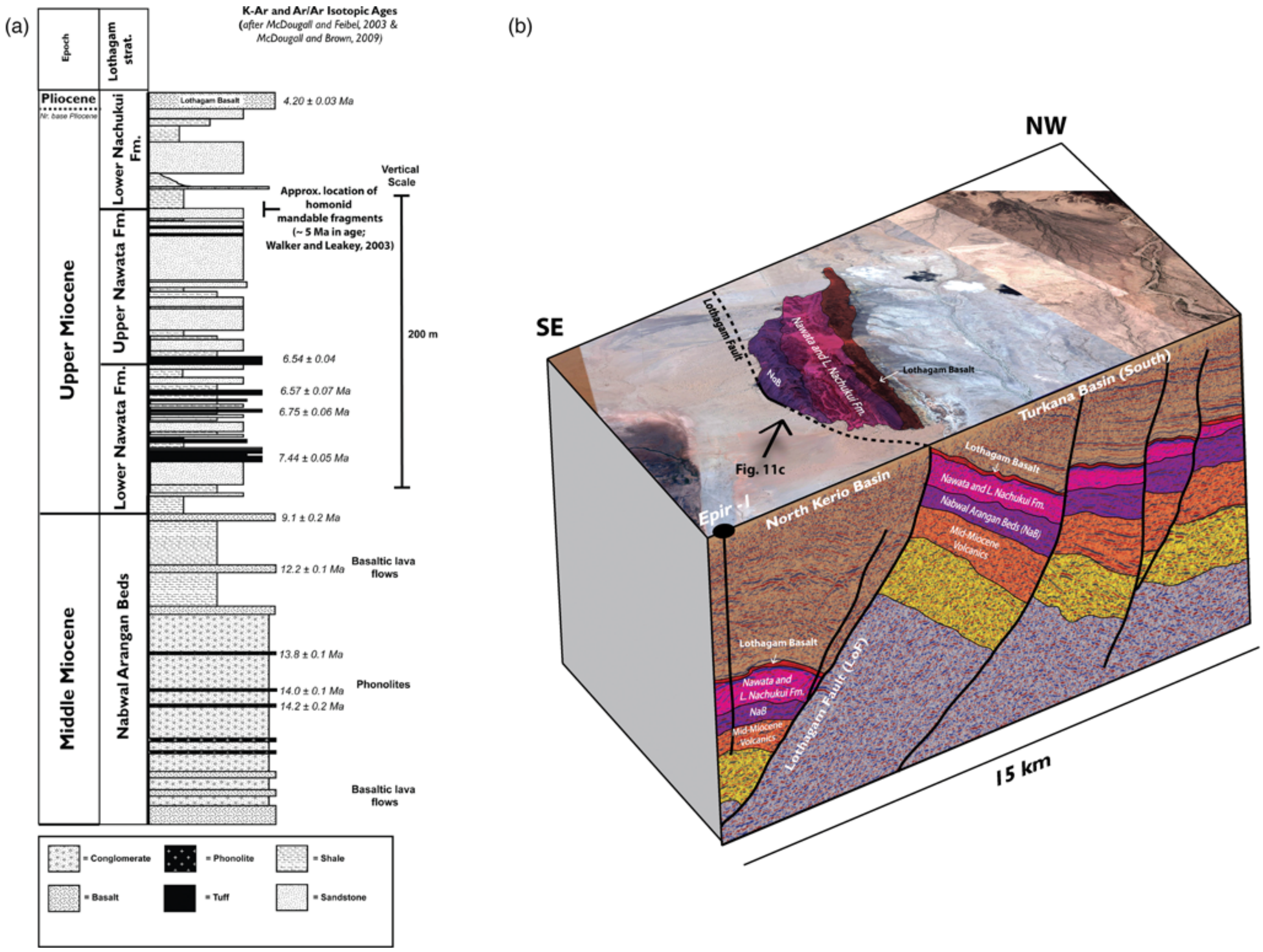

Fig. 12. (**a**) Stratigraphy of Lothagam (modified from McDougall and Feibel 1999; McDougall and Brown 2009). Note the phonolites within the Nabwal Arangan beds. (**b**) Geo-seismic block diagram showing the relationship of Lothagam to the subsurface footwall block and Epir-1 well, drilled 7 km away.

the Nachukui Formation whose lower sequences comprise a series of fluvial to lacustrine sequences that pass into dominantly lacustrine mudstones towards the top of the formation (Fig. 12a).

The Pliocene-aged Lothagam Basalt (4.20 Ma ± 0.2 Ma, McDougall and Feibel 1999), within the Lower Nachukui Formation (Fig. 12a) (Leakey *et al.* 1996), forms a prominent

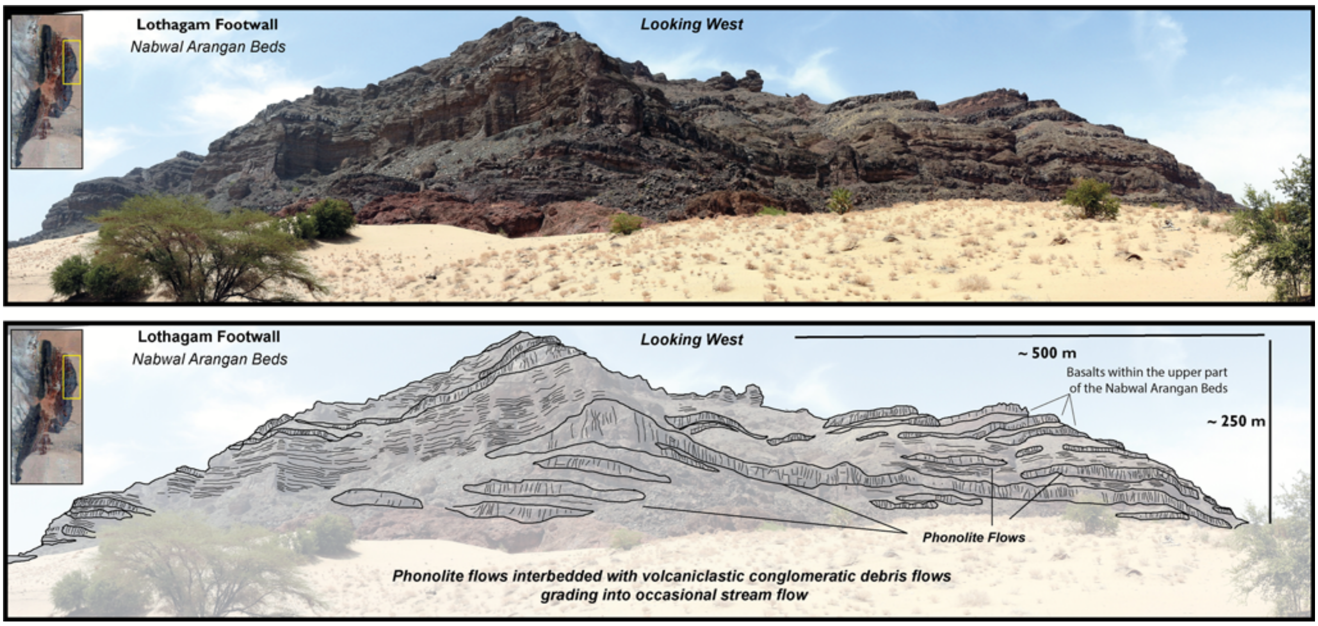

Fig. 13. Field photograph and overlay showing the nature of the Nabwal Arangan beds in Lothagam, which consist of compound braided phonolite flows interbedded with volcaniclastic conglomeratic debris flows. Three basaltic lavas occur towards the top of the sequence.

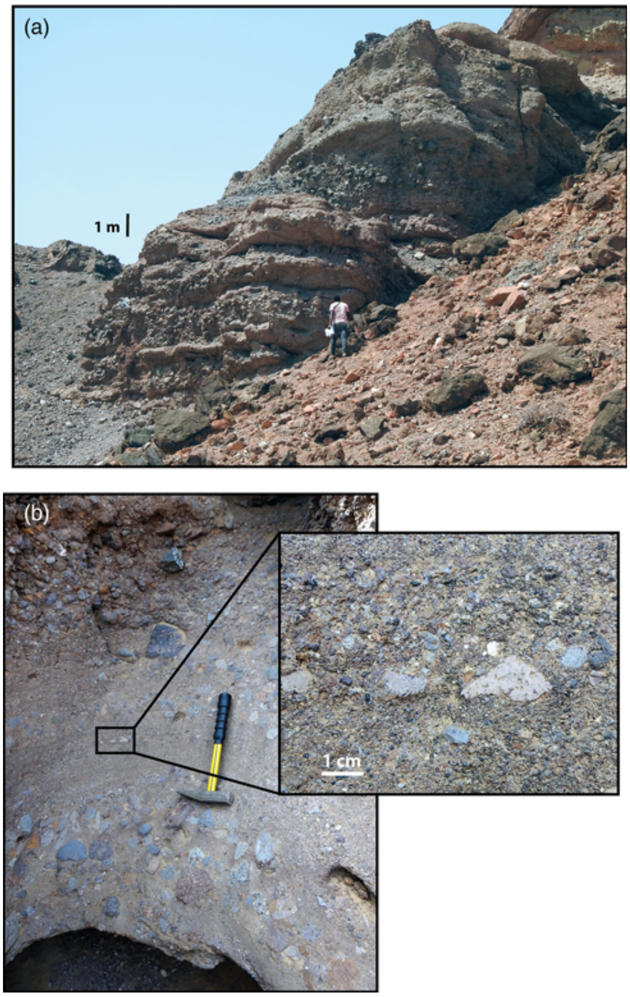

Fig. 14. (**a**) Close-up view of the volcaniclastics of the Nabwal Arangan beds; note the boulder size of the clasts and alluvial fan-type deposits. (**b**) Grading within the Nabwal Arangan beds within an inset photo showing the range of volcanic lithologies visible within the beds, which consist of basalt, phonolite and other alkali rock clasts.

topographic feature that extends along the strike of the exposure (Fig. 11). Whether the basalt is intrusive or extrusive has been debated previously (Patterson *et al.* 1970). However, the unit can be traced into the subsurface on the seismic data (Figs 8 and 16), where it is conformable with the surrounding strata. This unit is also penetrated by Epir-1 (North Kerio Basin) and Eliye Springs-1 (Turkana Basin) (see the following sections), suggesting that it represented an aerially extensive basaltic tabular lava flow that covered much of the Turkana area. This is also supported by McDougall and Feibel (1999) who interpret the Lothagam basalt as a lava flow emplaced on top of soft sediment.

It is important to note that, although the highly detailed stratigraphy of Lothagam has been established (Powers 1980; McDougall and Feibel 1999; Feibel 2003), the broad stratigraphic relationship of the Lothagam stratigraphy regionally across the Turkana area from subsurface to surface outcrops, e.g. to the Napedet Hills and further afield into the North Lokichar and North Kerio Basins, has not been previously established in detail.

North Kerio Basin (Epir-1)

The Epir-1 well was drilled within the North Kerio Basin in 2014 by Tullow Oil plc. and Africa Oil Corp. The well, which sits 7 km to the north east of Lothagam, provides a key link between the surface stratigraphy of Lothagam and the subsurface stratigraphy of the North Kerio Basin (Fig. 12). The well reached a total depth of 3057 mBRT and penetrated two volcanic sequences (Fig. 15), the first near to the base Pliocene at 1505 mBRT and the second within the Miocene at 2220 mBRT. The detailed lithological and petrophysical analysis is presented in Figure 15. At 1505 mBRT, near the base Pliocene, two tabular lava flows (34 m and 7 m thick respectively), separated by a thin *c*. 1 m mudstone interbed were intersected. The well then penetrated a 640 m thick sequence of Upper Miocene interbedded sandstone and claystone before encountering a second, 813 m thick, volcanic sequence at 2220 mBRT, composed of extrusive volcanics, siliciclastic and volcaniclastic rocks. The top of the second volcanic section is marked by a 92 m thick package of tabular and compound lava flows. These flows directly overlay a 207 m thick volcaniclastic conglomerate section characterized by a very high gamma response (>150 API). Two SWCs within the sequence are composed of volcanic lithologies rich in potassium feldspar (Fig. 7), which explain the high gamma facies seen on the spectral gamma potassium log (Fig. 15).

Directly underlying the volcanic conglomerate and marked by a distinct change in the gamma-ray and resistivity logs at 2519 mBRT is a second, *c*. 520 m thick, package of lava flows, separated by claystone and thin occasional volcaniclastic horizons. At 2714 mBRT an 87 m thick package of lava flows occurs. The high gamma values (*c*. 100 API) and the increased separation on the neutron density log suggest a dacitic composition (no SWC was available over this interval). From 2826 mBRT to 3034 mBRT is a 208 m thick series of basaltic, tabular and compound braided lava flows (see Nelson *et al.* 2009), interbedded with claystone and volcaniclastics.

Turkana Basin (Eliye Springs-1)

The Eliye Springs-1 well was drilled by Shell in 1992 to a depth of 2964 mBRT within the Turkana Basin (Fig. 3) and represents the first well that was drilled within the western Turkana area. The well targeted a tilted fault block adjacent to the Napedet-Loperot Fault and encountered a Plio–Pleistocene to Upper Miocene sequence of mainly fluvio-lacustrine deposits (Fig. 16). The well intersected a 34 m thick volcanic section at 1888 mBRT, which corresponds to the near-base Pliocene. At 2895 mBRT, near the base of the well, a 55 m thick sequence of stacked lava flows with thin limestones, underlain by red claystone, was penetrated before the well reached TD.

Lothidok Ranges

West of the Eliye Springs-1 well, and north of the Napedet Hills, lie the Lothidok Ranges (Fig. 3). These consist of an extensive region of Late Oligocene–Middle Miocene volcanic and sedimentary rocks, composed of basaltic lava flows, tuffs, volcaniclastic conglomerates and sandstones (Boschetto *et al.* 1992). The following account of the geology is based on Boschetto (1988) and Boschetto *et al.* (1992). Two main volcanic sequences occur within the Lothidok Ranges; the Kalakol Basalts and Loperi Basalts, between which sits the Lothidok Formation. The Kalakol Basalts have a thickness ≥ 785 m and consist of a series of at least 20 separate basaltic lava flows ranging from 4 to 60 m in thickness, interbedded with volcaniclastics. The Kalakol Basalts have been dated to have erupted from the Late Oligocene to Early Miocene (*c*. 27.5 Ma to 17.9 Ma). The Lothidok Formation, which is defined as all the strata that lie between the top of the Kalakol Basalts and overlying Loperi Basalts (Boschetto *et al.* 1992) was deposited from the Late Oligocene into the Middle Miocene (*c*. 17.5 Ma to 13.2 Ma) and consists of 580 m of volcaniclastic sedimentary rock, with altered tuff horizons (Boschetto *et al.* 1992). Unconformably overlying the Lothidok Formation are the Loperi Basalts, which have been dated as Middle Miocene in age (*c*. 12.2 Ma)

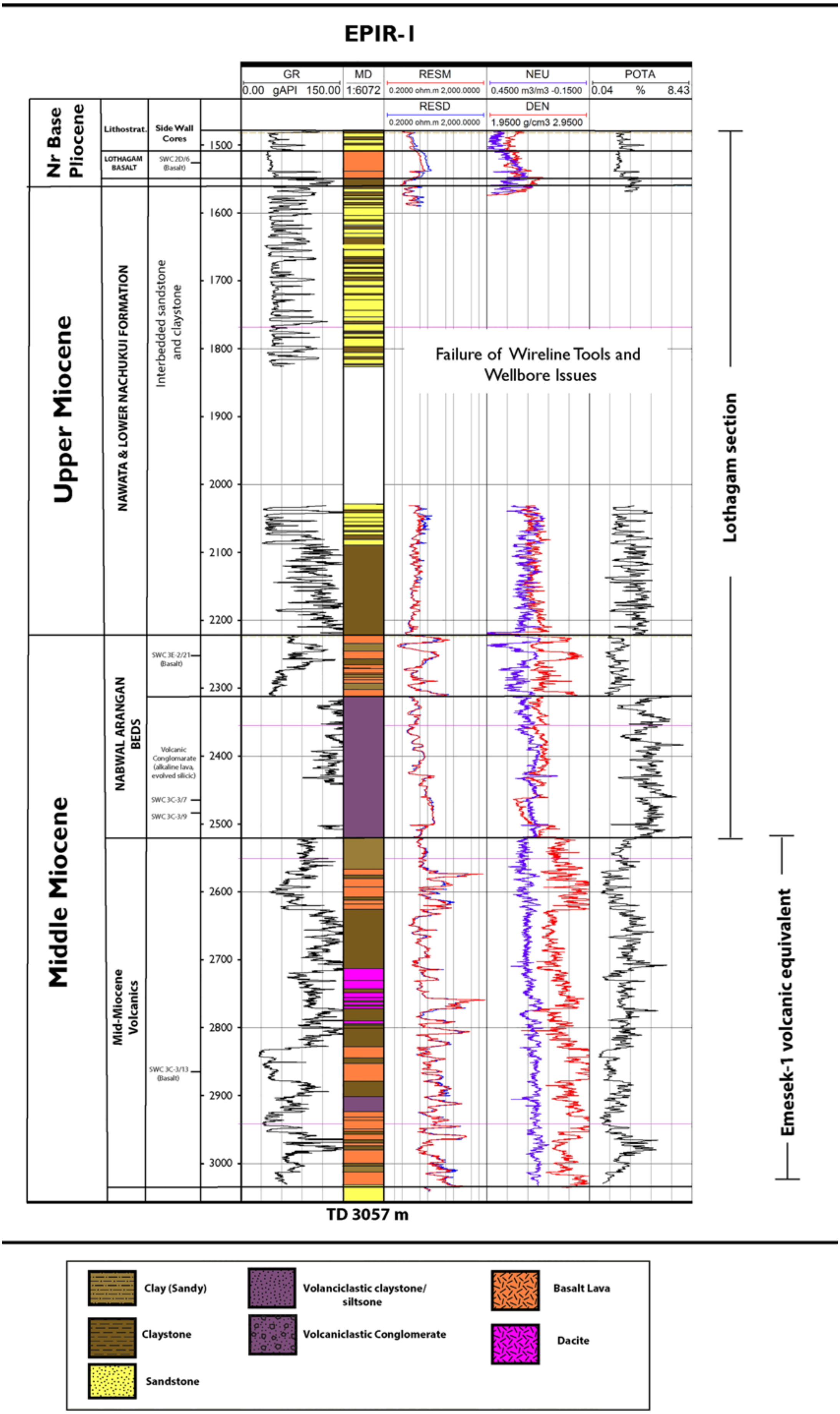

Fig. 15 . Epir-1 well logs showing the volcanic sequences penetrated that can be tied to the stratigraphy established by Powers and Feibel (in Leakey 1996) of Lothagam. The Nabwal Arangan beds form a petrophysically distinct unit which possesses a very high gamma value (>150 API), due to the high K–feldspar content of the volcaniclastics within the unit.

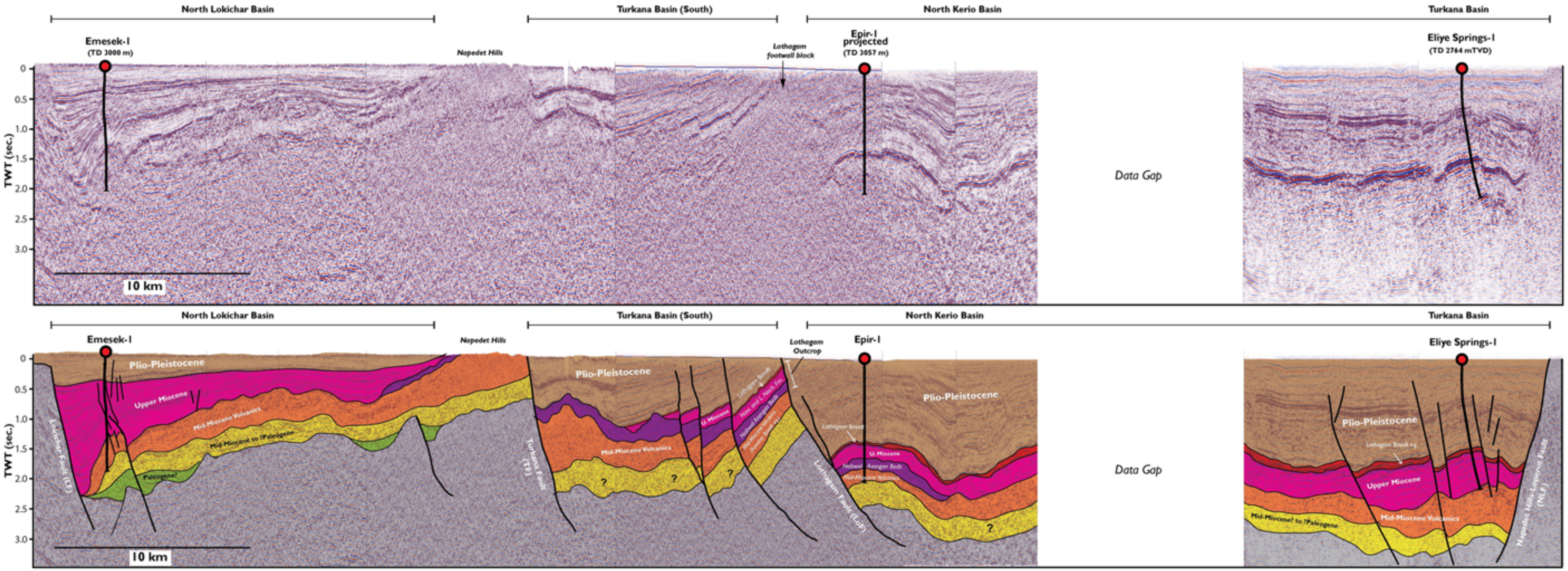

Fig. 16. Seismic and geo-seismic interpretation showing the correlation of Emesek-1, Epir-1 and Eliye Springs-1. Of note is that despite the gap in data, the near-base Pliocene-aged Lothagam Basalt can be successfully traced from the Lothagam footwall block, through Epir-1 and into Eliye Springs-1 in the Turkana Basin. The Middle Miocene volcanic unit is also interpreted to be present across the North Lokichar, Turkana (South), North Kerio and Turkana Basins. See Figures 3 and 4 for locations.

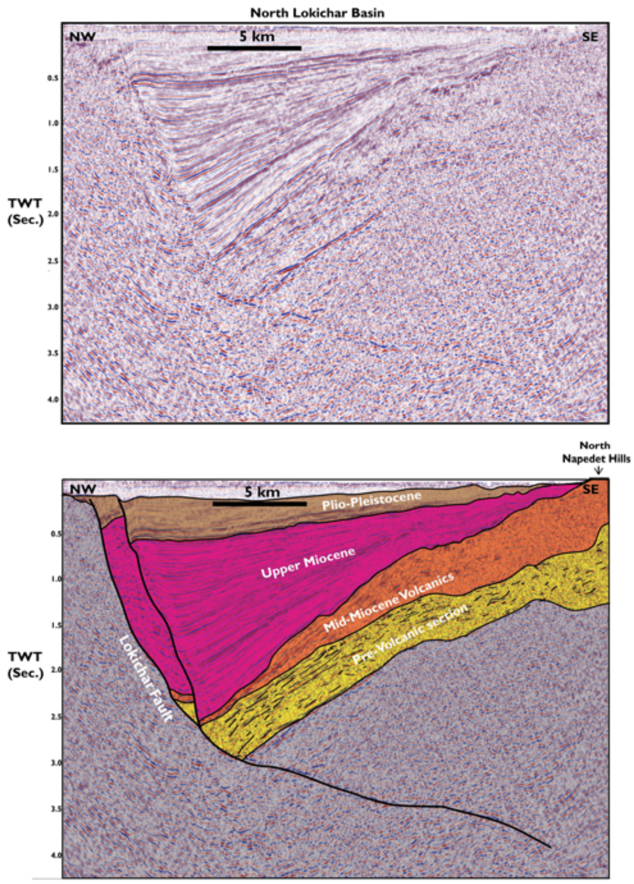

Fig. 17. Seismic line from the North Lokichar Basin, which shows uplift in imaging beneath the volcanics. The volcanics and pre-volcanic section, likely consisting of Middle Miocene strata, show generally strata-parallel reflection with no evidence of thickening into the Lokichar Fault, supporting the supposition that the volcanics were erupted in a pre-rift setting, prior to the main movement on the Lokichar Fault in the Upper Miocene.

and reach a maximum thickness of 121 m in exposed sections within the Lothidok Hills. At around 12 Ma volcanics from the Napedet Hills probably formed a continuous belt with those in the Lothidok Hills (Boschetto 1988). The Loperi Basalts likely represent the stratigraphic equivalent of the 55 m thick package of stacked lava flows penetrated towards the base of the Eliye Springs-1 well at 2895 mBRT.

Seismic interpretation and correlation of outcrop and subsurface volcanic sequences across the western Turkana Basins

Correlation of North Lokichar (Emesek-1) –Napedet Hills–Turkana Basin (South) –Lothagam–North Kerio Basin (Epir-1)

Using the available well, outcrop and new seismic data, it is possible to correlate the volcanic sequences from North Lokichar into the North Kerio Basin. The 781 m thick volcanic sequence penetrated by Emesek-1 can be seen on seismic reflection data to thin westwards towards the Lokichar Fault and to thicken eastwards, to *c.* 1350 m, towards the Napedet Hills (Figs 8 and 17). The volcanics penetrated by Emesek-1 broadly represent the same stratigraphic unit of volcanics that crop out within the Napedet Hills, although from the seismic reflection data notable erosion and truncation of the volcanic sequence appear to have occurred within the Napedet Hills, meaning that several hundred metres of volcanic sequence are likely to have been eroded (Figs 8 and 9).

The Napedet Hills volcanics are downthrown on their eastern margin by the Turkana Fault *c.* 1.5 km into the southern portion of the Turkana Basin. Within the Turkana Basin (South), immediately adjacent to the Turkana Fault, are three volcanic edifices which can be identified clearly on seismic reflection data (Figs 8, 10 and 16), and are onlapped by upper Miocene and Plio–Pleistocene sedimentary rocks. It is considered likely that these three edifices represent subsurface equivalents of the same microfoyaite igneous centres (although not as heavily eroded) seen extensively across the Napedet and Kamutile Hills (Fig. 10) (see Dodson 1971).

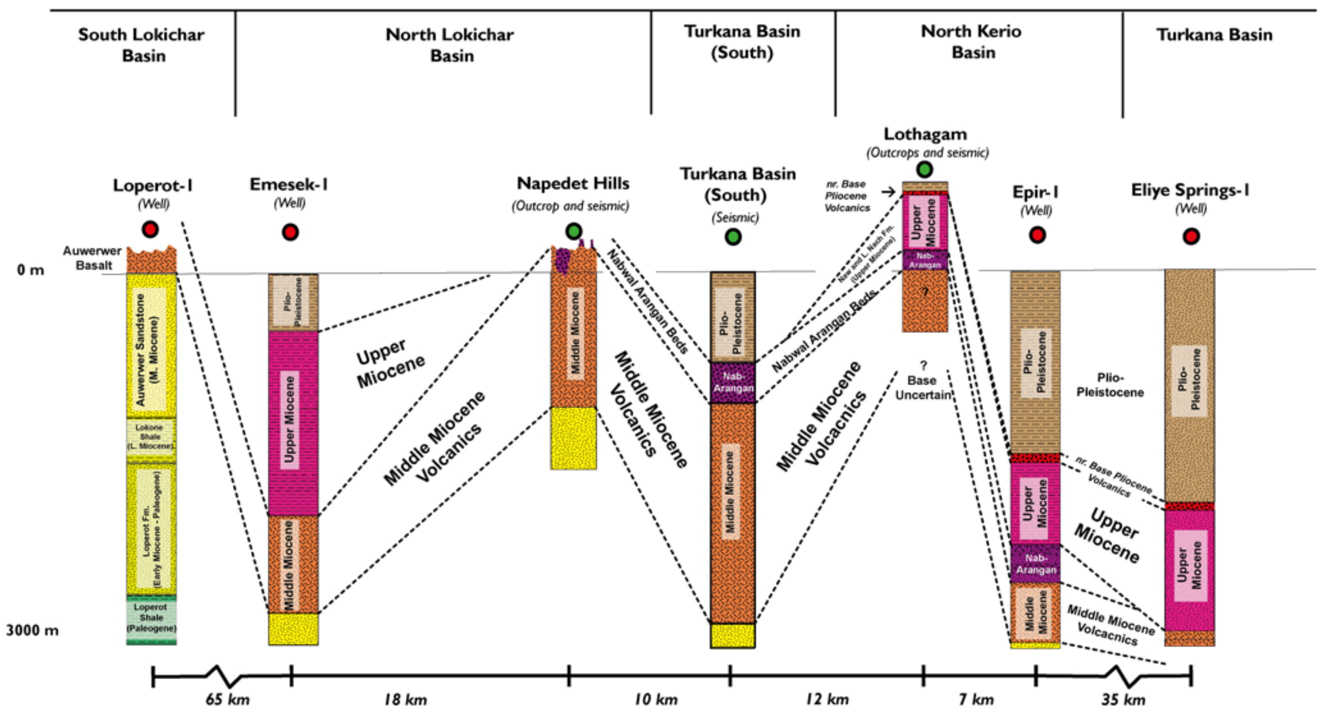

Fig. 18. Correlation across the study area based on well, seismic and outcrop. Loperot-1 well stratigraphy after Morley *et al.*, (1999).

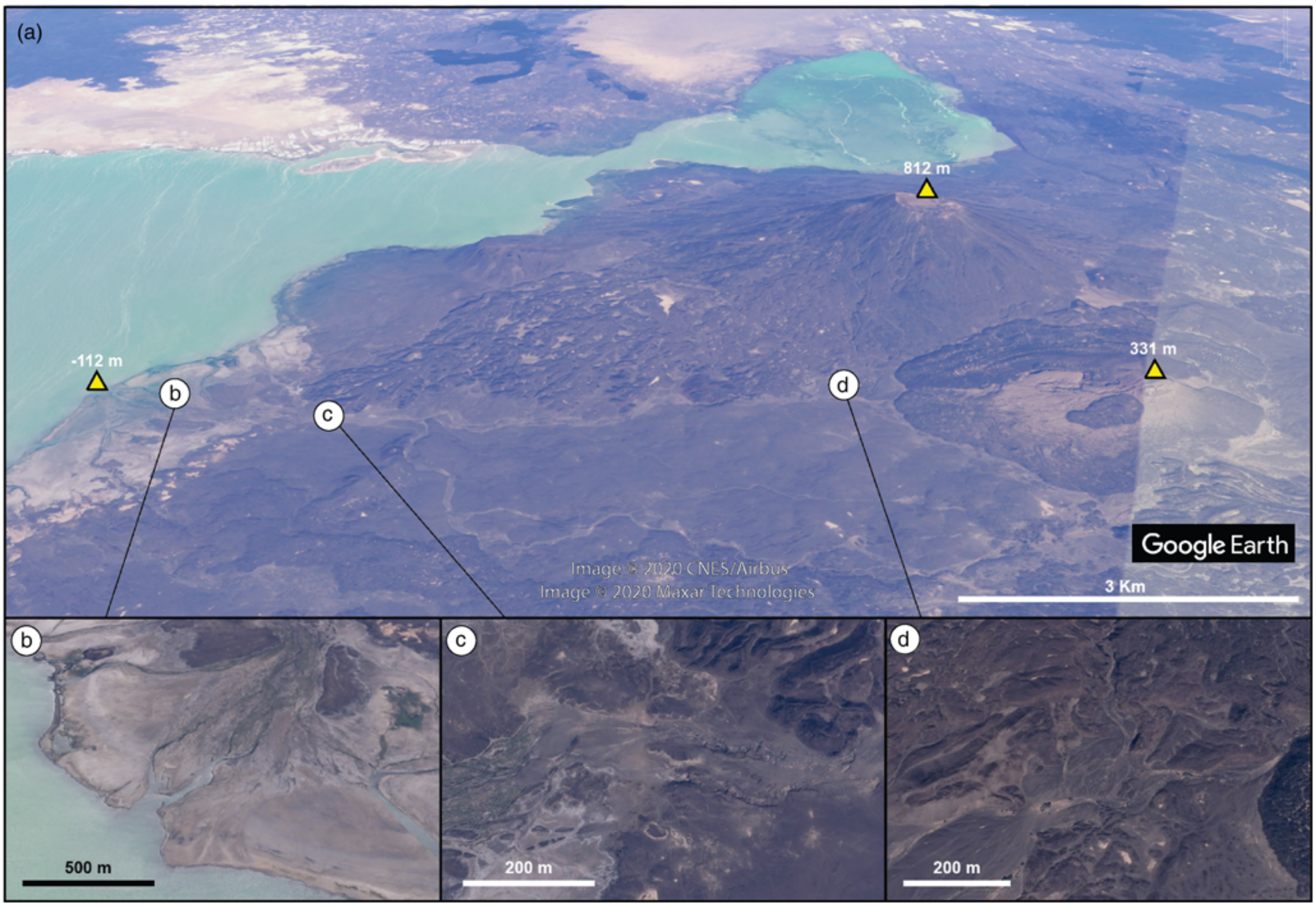

Fig. 19. Sedimentary systems associated with the Holocene-aged Borawli Volcano in Ethiopia. (**a**) Oblique view looking northwest; note the topography that is created by the edifice and associated lava field alone, with no tectonic uplift. (**b**) Distal alluvial/fluvial distributary fan system, similar to the facies seen within the Nabwal Arangan beds of Lothagam. (**c**) A channelized high-energy fluvial system can effectively break down volcanic material. (**d**) High-energy confined edifice flank systems dominantly conglomeratic in nature. The fluvial systems associated with the unconfined flood plain are also likely dominated by coarse to conglomeratic deposits. Images from Google Earth (*Google Earth;* earth.google.com/web/)

Correlation of Lothagam to North Kerio Basin (Epir-1)

Lothagam and Epir-1 provide an important stratigraphic context to link the surface geology to subsurface seismic interpretation of the North Kerio Basin, as it can be shown that the detailed stratigraphy developed for Lothagam (see Feibel 2003) can be successfully traced into the subsurface via both well and seismic reflection data (Figs 15, 16 and 18). Lothagam contains the geologically distinctive Nabwal Arangan beds at its base, which are composed of phonolite flows, alkali lava, and volcaniclastic sequences, and contain a large volume of potassic-rich volcanic material (McDougall and Brown 2009). The Epir-1 well, located 7 km to the NE of Lothagam, also intersected a distinctive high potassium unit, with gamma-ray log values exceeding 150 API units. SWCs taken within this unit confirms that it is composed of volcaniclastic material containing alkali-rich lava fragments analogous to the Nabwal Arangan beds (Fig. 7). The high-gamma potassic volcanics recognized in the Epir-1 well can be traced on the seismic reflection data to the Lothagam Fault and are interpreted to correlate with comparable lithologies in the Nabwal Arangan beds exposed on the uplifted footwall block.

Given the well-defined correlation of the Nabwal Arangan beds between Lothagam and Epir-1, the basaltic tabular lava flows penetrated in Epir-1 at 1505 mBRT (Fig. 15), which form the prominent high-amplitude seismic marker at *c.* 1.5 s TWT (Fig. 16), is interpreted to represent the near-base Pliocene-aged Lothagam Basalt.

The Middle Miocene volcanic package encountered in Epir-1 (below the Nabwal Arangan beds) (Fig. 15), which consists of a *c.* 520 m thick sequence of basaltic lava flows, claystone and thin occasional volcaniclastic horizons, is not fully exposed within the Lothagam footwall (Figs 15 and 18). Within Epir-1, the top of the Middle Miocene volcanic package is characterized by a series of basaltic flows lava at *c.* 2600 m depth (Fig. 15). These lava flows may correlate to the basaltic lava flows seen at the base of the Nabwal Arangan beds in Lothagam (Fig. 12a).

Although seismic interpretation of the Middle Miocene volcanic unit is challenging, due to the overlying volcanic sequences of the Nabwal Arangan beds hindering the seismic imaging, it is tentatively interpreted that the Middle Miocene volcanics penetrated by Emesek-1 link with the volcanic sequences that outcrop within the Napedet and Kamutile Hills (Figs 16 and 18). This interpretation is also supported by the observation that the lower volcanic package in Epir-1 shares similar lithological and stratigraphic relationships to the volcanic sequence penetrated by Emesek-1, namely two basaltic eruptive episodes separated by a more volcanically evolved dacitic eruptive episode.

Correlation to Eliye Springs-1

A lack of seismic reflection data coverage makes confident seismic correlation of Epir-1 (North Kerio Basin) and Eliye Springs-1 (Turkana Basin) relatively challenging. However, seismic data do show that there is seismic stratigraphic continuity between the volcanic sequences penetrated by Epir-1 into Eliye Springs-1 (Fig. 16). The near-base Pliocene tabular basalt sequence penetrated within Epir-1 (Fig. 15), which is also the stratigraphic equivalent of the Lothagam Basalt (Figs 11 and 12), can be traced on seismic

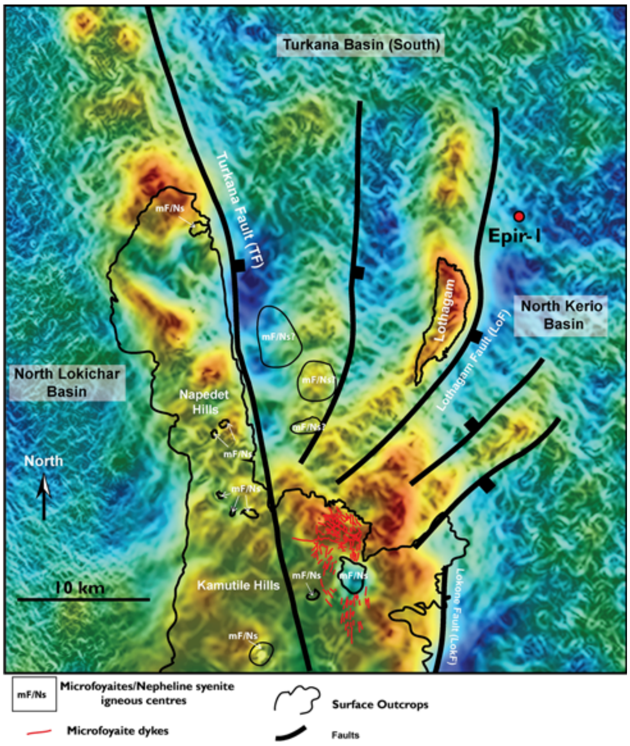

Fig. 20. Full-tensor gradiometry image of Napedet Hills, Kamutile Hills and Lothagam, showing therelationship of faulting. Note the splaying of faulting which occurs away from the Kamutile Hills and Turkana Fault.

reflection data to the basalt that was penetrated at 1893 mBRT in the Eliye Springs-1 well, which is represented by a very bright seismic amplitude event at *c.* 1.5 s TWT (Fig. 16).

Towards the base of Eliye Springs-1, the well only partly penetrated into a volcanic sequence which, from the seismic correlation, seems likely to be the seismic stratigraphic equivalent to the top of the Middle Miocene volcanic sequences penetrated in Epir-1 (Figs 16 and 18).

Discussion

Relationship of the volcanic sequences across the North Lokichar, Turkana and North Kerio Basins

The Middle Miocene volcanics penetrated by Emesek-1 in the North Lokichar Basin show no thickening relationship towards the main Lokichar Fault (Figs 8 and 17), but instead thicken considerably towards the present-day location of the Napedet Hills and Turkana Fault, reaching a thickness of *c.* 1800 m on the downthrown section of the Turkana Fault (Fig. 8). The lack of thickening of the volcanics (but substantial syn-rift thickening of the overlying Upper Miocene sediments into the Lokichar Fault) provides compelling evidence that the volcanic sequence itself was erupted in a pre-rift setting prior to the formation of the North Lokichar Basin (Morley *et al.* 1999). The Middle Miocene sedimentary sequence that underlies the extrusive volcanic sequence within the North Lokichar Basin is characterized by a series of largely strata-parallel reflectors, displaying no apparent thickening against the Lokichar Fault, again suggesting that both Middle Miocene sedimentary and volcanic sequence within the North Lokichar Basin were not deposited in a syn-rift setting and that the main movement on Lokichar Fault occurred in the Upper Miocene (Fig. 17). This further confirms the interpretation of Morley *et al.* (1992), who suggested that the main phase of extension and half-graben formation within the North Lokichar Basin began in the Upper Miocene, in contrast to the South Lokichar Basin, which shows substantial Mid-Miocene and earlier rifting episodes (Morley *et al.* 1992). Therefore it is likely due to the lack of faulting and accommodation that the pre-volcanic sedimentary unit, penetrated by Emesek-1, underlying the extrusive volcanics within the North Lokichar Basin represents a condensed time-equivalent section to the Middle Miocene Auwerwer Sandstone Formation (and potentially older sections), found beneath the Middle Miocene volcanics of the South Lokichar Basin.

Within the Turkana Basin (South) and into the North Kerio Basin, to the east of the Napedet Hills, the volcanic sequence penetrated by Emesek-1 and exposed in the Napedet Hills is downthrown against the Turkana Fault and eastwards again by the Lothagam Fault (Fig. 8). The main phase of rifting and basin formation within the Turkana Basin (South) and North Kerio Basin appears to have begun in the Plio–Pleistocene, with syn-rift thickening observable within the Plio–Pleistocene sequences towards the Turkana and Lothagam Fault. Importantly, the Upper Miocene and Plio–Pleistocene onlap onto the underlying Middle Miocene volcanic sequences, including the volcanic edifices identified within the Turkana (South) Basin, suggests that through the Upper Miocene and into the Plio–Pleistocene the volcanic sequences were exposed and likely eroding volcanic material into the Turkana and North Kerio Basins.

As observed in Lothagam, Epir-1 and Eliye Springs, the near-base Pliocene is marked by a regionally extensive but relatively thin tabular lava sequence (Fig. 8, 11, 12, 15, 16 and 18). Similar to the extensive pre-rift Middle Miocene volcanism seen across the Turkana area, the near-base Pliocene volcanic sequences across the southern Turkana depression also appear to represent a pre-extension phase volcanic sequence, with Pliocene rifting subsequently initiating within the Turkana and the North Kerio Basins after its eruption.

Volcanic stratigraphy of Emesek-1, Epir-1 and Nabwal Arangan beds

The Emesek-1 and Epir-1 wells give important subsurface datapoints to understand the broad subsurface volcanic stratigraphy in the North Lokichar and North Kerio Basins, and the relationship to volcanics exposed at surface (e.g. Napedet Hills and Lothagam), especially when these wells are placed in context of regional seismic lines (Figs 16 and 18).

Although Emesek-1 and Epir-1 (Figs 6 and 15) are now located in separate sub-basins, during the Middle Miocene this was not the case, as rifting took place in the North Lokichar during the Upper Miocene and in the North Kerio Basin during Plio–Pleistocene. Importantly, the volcanic stratigraphy in both wells suggests a general common volcanic stratigraphy initially developed across the North Lokichar and North Kerio Basins. The base of the volcanic sequence in Emesek-1 is characterized by a series of tabular basaltic lava flows. The base of the volcanic sequences in Epir-1 is also characterized by a series of tabular and compound basaltic lavas. Emesek-1 is then overlain by a series of dacitic lavas, which are interpreted to also occur in Epir-1 in the same context (i.e. dacite overlying basalt). The dacite lavas are then overlain by basaltic lavas in both wells. It therefore seems that, within the North Lokichar and Northern Kerio Basins, the Middle Miocene pre-rift volcanism was dominated by an initial phase of basaltic magmatism, followed by a more evolved phase, before basaltic volcanism resumed. In the North Lokichar Basin, this appears to constitute the main phase of volcanism, but eastwards towards the Napedet Hills, Lothagam and in Epir-1, evidence of substantial alkali volcanism occurs. The pronounced phonolite flows and alkali-rich volcaniclastics that dominate the Nabwal Arangan beds in Lothagam can be confidently tied between the outcrops at Lothagam into the Epir-1 well and the subsurface of the North Kerio Basin.

The Nabwal Arangan beds were dated by McDougall and Feibel (1999) as being deposited from Middle to Upper Miocene (*c*. 15 Ma to 9 Ma), and therefore the underlying, mainly basaltic, Middle Miocene volcanic unit that was intersected in Emesek-1 (North Lokichar) and Epir-1 (North Kerio Basin) could be broadly assigned to the same volcanic package.

The alluvial fan facies and intercalated compound lava flows of the Nabwal Arangan beds indicate that high levels of erosion and sediment transport, interspersed with volcanic eruptions, dominated the Middle to Upper Miocene within the present-day location of the North Kerio and Turkana (South) Basins. A substantial fluvial system must have been in operation at this time, as the large boulder-sized volcanic clasts within the Nabwal Arangan beds (Fig. 14) show a high degree of rounding, presumably as a result of fluvial transport prior to deposition in the alluvial fan system. Similar complex volcano-sedimentary relationships, which show an interaction between fluvial and alluvial systems, in conjunction with contemporaneous volcanism, can be seen in the present day within the EARS (Fig. 19). These systems highlight the substantial topography (and sedimentary system) that an extrusive volcanic system can create without the need for tectonic uplift-related topography. It is envisaged that the Nabwal Arangan beds were deposited in a similar style to the systems shown within Figure 19, where the topography created by both the volcanic flows and volcanic edifices, now located within the present-day Napedet and Kamutile Hills, as well as edifices identified within the subsurface Turkana (South) Basin, led to a highly active sedimentary system that shed volcaniclastic material into and away from the lava field via fluvial systems and alluvial fans.

Factors that concentrated volcanism and its relation to rifting

Within the North Lokichar, Turkana (South) and North Kerio Basins, the Middle Miocene volcanism and later sites of Plio–Pleistocene rifting appears to have centralized around the Napedet and Kamutile Hills, which is demonstrated by the thickening relationships of the extrusive volcanic sequences and presence of numerous igneous centres and dyke swarms (Figs 10 and 20) (Dodson 1971). The main movement on the Turkana Fault occurred during the lower Pliocene which is *c.* 5 Ma after the Middle Miocene volcanic phase ceased.

On gravity data, towards the east of the Napedet Hills, the Plio–Pleistocene faults system, including the Turkana Fault and Lothagam Fault, appears to converge in a southward direction towards an area in the Kamutile Hills (Fig. 20). This area of convergence shows a complex array of microfoyaite dyke swarms and several microfoyaite igneous centres (Fig. 20) (Dodson 1971; Morley 2020). It therefore seems likely that the same crustal weaknesses, or crustal structure, that may have acted as preferential conduits to the magma eruption and intrusion of volcanics in and away from the Napedet and Kamutile, also acted as preferential zones for Pliocene and later rifting to initiate within the Turkana Basin (South) and North Kerio Basins.

Conclusions

In this paper the subsurface volcanic stratigraphy of the North Lokichar, North Kerio and Turkana Basins has been examined and placed in stratigraphic context against key surface outcrops of the Napedet Hills and Lothagam.

- The Emesek-1 well, drilled within the North Lokichar Basin, penetrated *c*. 700 m of tabular basaltic lavas and a more evolved dacite package.
- Emesek-1 also intersected a 200m+ thick package of sub-volcanic sandstones which contained little freshly derived volcanic material.
- The highly detailed stratigraphy of Lothagam forms an important data point that can be successfully extrapolated into the subsurface of the North Kerio and Turkana (South) Basins via the Epir-1 well, where the characteristic Nabwal Arangan beds present in Lothagam can be identified on wireline logs.
- The site of the Plio–Pleistocene-aged Turkana Fault appears to have initiated along the same area that Middle Miocene volcanism was focused, with the Kamutile Hills appearing to have acted as a focus both for Middle Miocene intrusive and extrusive volcanism, and later Plio–Pleistocene faulting.
- The Middle Miocene volcanism encountered in the Emesek-1 well, which also outcrops within the Napedet and Kamutile Hills, appears to have erupted in a pre-rift setting, prior to the main initiation of faulting on the North Lokichar Fault during the Upper Miocene.

Acknowledgments The Kenyan JV (Tullow Oil, Africa Oil and Total) are thanked for allowing publication of this paper. Views expressed within this paper by authors are not necessarily the views of the Kenyan JV. Seismic and Well Interpretation was undertaken using Schlumberger Petrel and Techlog Software. ALS Petrophysics is acknowledged for thin section petrography of Epir-1 in Figure 7. Stuart Archer is thanked for discussions with regard to rift stratigraphy. We would like to thank Simon Holford and Craig Feibel for reviews which considerably helped improve this paper. Tyrone O. Rooney is thanked for editorial guidance. Dennis Wairimu and Francis Karanja are thanked for accompanying in the field. The Kapese *Camp and* Drivers are thanked for accommodating the fieldwork in a very professional manner. Mark Goodchild is thanked for facilitating fieldwork and research funding.

Author contributions **NS**: conceptualization (lead), data curation (lead), investigation (lead), methodology (lead), visualization (lead), writing–original draft (lead), writing–review & editing (lead); **RN**: conceptualization (supporting), investigation (supporting), writing–original draft (supporting), writing–review & editing (supporting); **ST**: conceptualization (supporting), data curation (supporting), investigation (supporting), writing–original draft (equal), writing–review & editing (equal); **DW**: conceptualization (supporting), data curation (supporting), formal analysis (equal), visualization (equal); **DWJ**: conceptualization (supporting), formal analysis (equal), writing–review & editing (supporting); **CM**: validation (supporting), writing–review & editing (supporting)

Funding The Kenyan JV are thanked for providing research funding for the project.

Data availability statement The data used in this study came from the Kenya JV (Tullow, Total and Africa Oil). Restrictions apply to the availability of these data, which were used under licence for the current study, and so are not publicly available.

Scientific editing by Tyrone Rooney

References

Baker, B.H., Mohr, P.A. and Williams, L.A.J. 1972. Geology of the Eastern Rift System of Africa. *Geological Society of America Special Paper*, **136**, 67.

Boone, S.C., Kohn, B.P., Gleadow, A.J., Morley, C.K., Seiler, C. and Foster, D.A. 2019. Birth of the East African Rift System: Nucleation of magmatism and strain in the Turkana Depression. *Geology*, **47**, 886–890, https://doi.org/10.1130/G46468.1

Boschetto, H.B. 1988. *Geology of the Lothidok Range, Northern Kenya*. Master's thesis, Department of Geology and Geophysics, University of Utah.

Boschetto, H.B., Brown, F.H. and McDougall, I. 1992. Stratigraphy of the Lothidok Range, northern Kenya, andK/Ar ages of its Miocene primates. *Journal of Human Evolution*, **22**, 47–71, https://doi.org/10.1016/0047-2484(92)90029-9

Davidson, A. and Rex, D.C. 1980. Age of volcanism and rifting in southern Ethiopia. *Nature*, **283**, 657–658, https://doi.org/10.1038/283657a0

Dodson, R.G. 1971. *Geology of the Area South of Lodwar: Degree Sheet 18, NE Quarter, with Coloured Geological Map(No. 87)*. Ministry of Natural Resources, Republic of Kenya.

Ebinger, C.J. 1989. Tectonic development of the Western Branch of the East African rift system. *Geological Society of America Bulletin*, **101**, 885–903, https://doi.org/10.1130/0016-7606(1989)101<0885:TDOTWB>2.3.CO;2

Ebinger, C.J. and Ibrahim, A. 1994. Multiple episodes of rifting in Central and East Africa: A re-evaluation of gravity data. *Geologische Rundschau*, **83**, 689–702, https://doi.org/10.1007/BF00251068

Ebinger, C.J. and Sleep, N.H. 1998. Cenozoic magmatism throughout east Africa resulting from impact of a single plume. *Nature*, **395**, 788, https://doi.org/10.1038/27417

Ebinger, C.J., Keir, D. *et al.* 2017. Crustal structure of active deformation zones in Africa: Implications for global crustal processes. *Tectonics*, **36**, 3298–3332, https://doi.org/10.1002/2017TC004526

Feibel, C.S. 2003. Stratigraphy and depositional history of the Lothagam sequence. *In*: *Lothagam: The Dawn of Humanity in Eastern Africa*. Columbia University Press, New York, 17–29.

Furman, T., Bryce, J.G., Karson, J. and Iotti, A. 2004. East African Rift System (EARS) plume structure: insights from Quaternary mafic lavas of Turkana, Kenya. *Journal of Petrology*, **45**, 1069–1088, https://doi.org/10.1093/petrology/egh004

Furman, T., Kaleta, K.M., Bryce, J.G. and Hanan, B.B. 2006. Tertiary mafic lavas of Turkana, Kenya: constraints on East African plume structure and the occurrence of high-μ volcanism in Africa. *Journal of Petrology*, **47**, 1221–1244, https://doi.org/10.1093/petrology/egl009

George, R. and Rogers, N. 2002. Plume dynamics beneath the African plate inferred from the geochemistry of the Tertiary basalts of southern Ethiopia. *Contributions to Mineralogy and Petrology*, **144**, 286–304, https://doi.org/10.1007/s00410-002-0396-z

George, R., Rogers, N. and Kelley, S. 1998. Earliest magmatism in Ethiopia: Evidence for two mantle plumes in one flood basalt province. *Geology*, **26**, 923–926, https://doi.org/10.1130/0091-7613(1998)026<0923:EMIEEF>2.3.CO;2

Haileab, B., Brown, F.H., McDougall, I. and Gathogo, P.N. 2004. Gombe Group basalts and initiation of Pliocene deposition in the Turkana depression, northern Kenya and Southern Ethiopia. *Geological Magazine*, **141**, 41–53, https://doi.org/10.1017/S001675680300815X

Hendrie, D.B., Kusznir, N.J., Morley, C.K. and Ebinger, C.J. 1994. Cenozoic extension in northern Kenya: A quantitative model of rift basin development in the Turkana region. *Tectonophysics*, **236**, 409–438, https://doi.org/10.1016/0040-1951(94)90187-2

Leakey, M.G. and Walker, A. 2003. The Lothagam hominids. *In*: *Lothagam: the dawn of humanity in eastern Africa*. Columbia University Press, New York, 249–257.

Leakey, M.G., Feibel, C.S. *et al.* 1996. Lothagam: a record of faunal change in the Late Miocene of East Africa. *Journal of Vertebrate Paleontology*, **16**, 556–570, https://doi.org/10.1080/02724634.1996.10011339

Mark, N.J., Schofield, N. *et al.* 2018. Igneous intrusions in the Faroe Shetland basin and their implications for hydrocarbon exploration; new insights from well and seismic data. *Marine and Petroleum Geology*, **92**, 733–753, https://doi.org/10.1016/j.marpetgeo.2017.12.005

McDougall, I. and Brown, F.H. 2009. Timing of volcanism and evolution of the northern Kenya Rift. *Geological Magazine*, **146**, 34–47, https://doi.org/10.1017/S0016756808005347

McDougall, I. and Feibel, C.S. 1999. Numerical age control for the Miocene-Pliocene succession at Lothagam, a hominoid-bearing sequence in the northern Kenya Rift. *Journal of the Geological Society, London*, **156**, 731–745, https://doi.org/10.1144/ gsjgs.156.4.0731). https://doi.org/10.1144/gsjgs.156.4.0731

Mechie, J., Keller, G.R., Prodehl, C., Khan, M.A. and Gaciri, S.J. 1997. A model for the structure, composition and evolution of the Kenya rift. *Tectonophysics*, **278**, 95–119, https://doi.org/10.1016/S0040-1951(97)00097-8

Millett, J.M., Wilkins, A.D. *et al.* 2016. The geology of offshore drilling through basalt sequences: Understanding operational complications to improve efficiency. *Marine and Petroleum Geology*, **77**, 1177–1192, https://doi.org/10.1016/j.marpetgeo.2016.08.010

Morley, C.K. 1994. Interaction of deep and shallow processes in the evolution of the Kenya rift. *Tectonophysics*, **236**, 81–91, https://doi.org/10.1016/0040-1951(94)90170-8

Morley, C.K. 2020. Early syn-rift igneous dike patterns, northern Kenya Rift (Turkana, Kenya): Implications for local and regional stresses, tectonics and magma-structure interactions. *Tectonics*, **16**, doi.org/10.1130/GES02107.1

Morley, C.K., Wescott, W.A., Stone, D.M., Harper, R.M., Wigger, S.T. and Karanja, F.M. 1992. Tectonic evolution of the northern Kenyan Rift. *Journal of the Geological Society*, **149**, 333–348, https://doi.org/10.1144/gsjgs.149.3.0333

Morley, C.K., Karanja, F.M., Wescott, W.A., Stone, D.M., Harper, R.M., Wigger, S.T. and Day, R.A. 1999. AAPG Studies in Geology# 44, Chapter 2: Geology and Geophysics of the Western Turkana Basins, Kenya.

Muirhead, J.D., Kattenhorn, S.A. *et al.* 2016. Evolution of upper crustal faulting assisted by magmatic volatile release during early-stage continental rift development in the East African Rift. *Geosphere*, **12**, 1670–1700, https://doi.org/10.1130/GES01375.1

Nelson, C.E., Jerram, D.A. and Hobbs, R.W. 2009. Flood basalt facies from borehole data: implications for prospectivity and volcanology in volcanic rifted margins. *Petroleum Geoscience*, **15**, 313–324, https://doi.org/10.1144/1354-079309-842

Patterson, B., Behrensmeyer, A.K. and Sill, W.D. 1970. Geology and fauna of a new Pliocene locality in north-western Kenya. *Nature*, **226**, 918, https://doi.org/10.1038/226918a0

Powers, D.W. 1980. *Geology of Mio-Pliocene sediments of the lower Kerio River Valley*. Ph.D. diss., Princeton University.

Ragon, T., Nutz, A., Schuster, M., Ghienne, J.F., Ruffet, G. and Rubino, J.L. 2018. Evolution of the northern Turkana Depression (East African Rift System, Kenya) during the Cenozoic rifting: New insights from the Ekitale Basin (28-25.5Ma). *Geological Journal*, **54**, 3468–3488, https://doi.org/10.1002/gj.3339

Rooney, T.O. 2017. The Cenozoic magmatism of East-Africa: Part 1 – Flood basalts and pulsed magmatism. *Lithos*, **286–287**, 264–301, https://doi.org/10.1016/j.lithos.2017.05.014

Rooney, T.O. 2020. The Cenozoic magmatism of East Africa: part V–magma sources and processes in the East African Rift. *Lithos*, **360**, 105296, https://doi.org/10.1016/j.lithos.2019.105296

Schofield, N., Holford, S., Edwards, A., Mark, N. and Pugliese, S. 2020. Overpressure transmission through interconnected igneous intrusions. *AAPG Bulletin*, **104**, 285–303, https://doi.org/10.1306/05091918193

Talbot, M.R., Morley, C.K., Tiercelin, J.-J., Le Herisse, A., Potdevin, J.-L. and Le Gall, B. 2004. Hydrocarbon potential of the Meso-Cenozoic Turkana Depression, northern Kenya. II. Source Rocks: Quality, maturation, depositional environments and structural control. *Marine and Petroleum Geology*, **21**, 63–78, https://doi.org/10.1016/j.marpetgeo.2003.11.008

Tiercelin, J.-J., Potdevin, J.-L., Morley, C.K., Talbot, M.R., Bellon, H., Le Gall, B. and Vetel, W. 2004. Hydrocarbon potential of the Meso-Cenozoic Turkana Depression, northern Kenya. I. Reservoirs: Depositional environments, diagenetic characteristics, and source rock-reservoir relationships. *Marine and Petroleum Geology*, **21**, 41–62, https://doi.org/10.1016/j.marpetgeo.2003.11.007

Tiercelin, J.-J., Potdevin, J.-L. *et al.* 2012*a*. Stratigraphy, sedimentology and diagenetic evolution of the Lapur Sandstone in northern Kenya: Implications for oil exploration of the Meso-Cenozoic Turkana depression. *Journal of African Earth Sciences*, **71–72**, 43–79, https://doi.org/10.1016/j.jafrearsci.2012.06.007

Tiercelin, J.-J., Nalpas, T., Thuo, P. and Potdevin, J.-L. 2012*b*. Hydrocarbon prospectivity in Mesozoic and early-middle Cenozoic rift basins of central and northern Kenya, Eastern Africa. *AAPG Memoir*, **100**, 179–207.

Vetel, W. and Le Gall, B. 2006. Dynamics of prolonged continental extension in magmatic rifts: the Turkana Rift case study (North Kenya). *Geological Society, London, Special Publications*, **259**, 209–233, https://doi.org/10.1144/GSL.SP.2006.259.01.17

Vetel, W., Le Gall, B. and Johnson, T.C. 2004. Recent tectonics in the Turkana Rift (North Kenya): An integrated approach from drainage network, satellite imagery and reflection seismic analysis. *Basin Research*, **16**, 165–181, https://doi.org/10.1046/j.1365-2117.2003.00227.x

Watson 2019. *Subsurface Characterisation of Igneous Rocks Within Regional Frameworks: Importance for Understanding Basin Volcanic Evolution & Hydrocarbon Exploration*. PhD Thesis, University of Aberdeen.

Ziolkowski, A., Hanssen, P. *et al.* 2003. Use of low frequencies for sub-basalt imaging. *Geophysical Prospecting*, **51**, 169–182, https://doi.org/10.1046/j.1365-2478.2003.00363.x